基于 CRISPR/Cas9 介导抗旱耐盐 *PagHyPRP1* 基因编辑杨树获得及抗性评价[1]

张伟溪[1#] 张腾倩[1,2#] 丁昌俊[1*] 胡赞民[3] 范成明[3] 张静[1] 李政宏[1] 沈乐[1] 张冰玉[1] 刘桂丰[2] 苏晓华[1*]

（1. 林木遗传育种国家重点实验室 国家林业和草原局林木培育重点实验室 中国林业科学研究院林业研究所 北京 100091；2. 林木遗传育种国家重点实验室 东北林业大学 哈尔滨 150040；3. 遗传与发育生物学研究所 中国科学院 北京 100101）

摘 要:【目的】由于干旱、半干旱和盐碱地区生态环境恶劣，植树造林和植被恢复困难，因此迫切需要创造抗逆林木新品种实现困难立地的栽培利用。**【方法】**本研究利用 CRISPR/Cas9 系统对模式树种 84K 杨（*Populus alba* × *P. glandulosa*）根部主要表达的盐和干旱胁迫响应负调控因子富含脯氨酸蛋白等位基因 *PagHyPRP1*（*PagHyPRP1A* 和 *PagHyPRP1B*）进行多位点基因组精准编辑。利用 PCR 产物测序和单克测序技术对编辑植株靶点进行编辑类型分析。通过氧化损伤水平、抗氧化和渗透调节能力对 4 种不同基因型编辑株系进行抗逆性评价，通过根系离子流速测定及根系离子转运相关基因表达分析解析编辑株系干旱和盐胁迫下 ROS 信号变化机制。**【结果】**共获得 9 株（5 种基因型）PagHyPRP1 编辑植株，编辑效率高达 60%，包括 2 个纯合、2 个等位基因突变和 5 个嵌合突变系。编辑位点编辑类型分析结果显示，靶点 1 bp 的插入或 1-4 bp 有效导致 *PagHyPRP1A* 和 *PagHyPRP1B* 蛋白质编码序列的移码突变。对 4 个靶点突变率 1000%的编辑植株（等位突变: prp-1; 纯合突变体: prp-2, prp-4; 嵌合突变体: prp-6）进行组培无性扩繁后检测发现，缺失结构稳定，无性繁殖并没有发生新的突变，因此选用这 4 个株系进行后续抗逆性评价。与野生 84K 相比，编辑株系的 *PagHyPRP1* 的表达水平无论在正常生长条件下还是盐和干旱胁迫下均显著低于，过表达 OE 株系的 *PagHyPRP1* 表达水平则相反，证实杨树 *PagHyPRP1* 基因在干旱和盐碱胁迫下的负调控作用。在干旱和盐胁迫下，*paghprp1* 突变株系株高、茎径、茎重、根干重和根冠比显著增加，耐盐性和抗旱性显著增强。此外，与 WT 对照相比，*paghyprp1* 突变株系表现出更高的超氧化物歧化酶（SOD）、过氧化物酶（POD）活性以及脯氨酸含量，更低的过氧化氢（H2O2）、超氧根离子（O2-）以及活性氧（ROS）的积累；较高的 Na^+外排（盐胁迫下）、Ca^{2+}内流量（干旱胁迫下）和 H^+内流量，更少的 K^+外排，而 OE 株系表现出相反的结果。说明 *paghyprp1* 突变株系可以通过提高 POD、SOD 等抗氧化酶活性、降低 ROS、H_2O_2 等活性氧的积累、减少细胞的膜质氧化程度、促进根系生长，同时维持根系 Na^+、K^+、H^+和 Ca^{2+}离子平衡，稳定根系渗透平衡，来提高编辑植物抗旱耐盐能力。**【结论】**本研究首次证实了杨树富含脯氨酸蛋白等位基因 *PagHyPRP1* 为盐和干旱胁迫响应负调控因子基因，*paghypp1* 突变株系通过减少 ROS 积累、促进根系生长和维持根系离子稳态来提高耐旱性和耐盐性。本研究为林木抗逆性基因编辑提供了具有重要育种价值的候选基因，为应用 CRISPR/Cas9 系统创造林木突破性抗逆性新种质提供了经验证据和技术参考。

关键词: CRISPR/Cas9, 杨树, HyPRP1,干旱胁迫, 盐胁迫, ROS, 离子流

基因项目: 1、“十四五”国家重点研发计划课题“林木良种高效遗传转化技术研究”（2021YFD2200102）；中国林业科学研究院中央级公益性科研院所基本科研业务费专项资金项目“高产高效型杨树种质创新与品种选育”（CAFYBB2020SZ002）；国家转基因新物种培育重大专项“转基因杨树新品种培育及产业化研究”（2018ZX08020002）

***通讯作者**：丁昌俊，E-mail: changjunding@caf.ac.cn 苏晓华；E-mail: suxh@caf.ac.cn

#：对论文贡献相同。

CRISPR/Cas9-mediated mutations of *PagHyPRP1* improves drought and salt tolerance in poplar[2]

Abstract: 【**Objective**】Due to the adverse ecological environment in arid, semi-arid and saline-alkali areas, afforestation and vegetation restoration are difficult. It is urgent to create new varieties of stress-resistant trees to realize the cultivation and utilization of difficult sites. 【**Method**】The CRISPR/Cas9 system was used for multilocus genome editing of *PagHyPRP1* (including alleles *PagHyPRP1A* and *PagHyPRP1B*), a negative regulator of salt and drought stress response in the important cultivated varieties *Populus alba* × *P. glandulosa* (84K poplar). PCR and single gram sequencing were used to analyze the editing type of editing targets. Oxidative damage level, antioxidant and osmoregulation capacity were measured in leaves to evaluate the tolerance to drought and salt stress of *PagHyPRP1*mutants. Key ion flux and related genes expression in roots were measured and analysed to investigate the ROS signalling alteration of the mutant in response to drought and salt stress. 【**Result**】9 mutant plants with 5 genotypes were obtained with 60% mutation efficiency, including two homozygous, two allelic, and five chimeric mutant lines. 1 bp insertion or 1-4 bp deletions that led to frameshift mutations were detected in mutants. The mutation type of four mutants (allelic mutant: prp-1; homozygous mutant: prp-2, prp-4; chimeric mutant: prp-6) with 100% mutation is stably, without the occurrence new mutations through asexual propagation, which were selected for drought and salt tolerance evaluation. Compared with 84K, the expression level of *PagHyPRP1* in mutants was significantly lower under normal growth conditions, salt and drought stress, which was opposite in OEs, suggesting that *PagHyPRP1* play the negative regulatory rol in poplar under drought and salt alkali stress. Under salt and drought stresses, the *paghyprp1* mutant lines showed significantly increased plant height, stem diameter, stem weight, root dry weight and root to shoot ratio than the wild-type 84K poplar, with significantly enhanced salt and drought tolerance. In addition, the *paghyprp1* mutant lines exhibited higher superoxide dismutase and peroxidase activities and proline content; lower accumulation of hydrogen peroxide, superoxide anions, and reactive oxygen species; higher Na^+ efflux (under salt stress), Ca^{2+} influx (under drought stress) and H^+ influx; and less K^+ efflux, while the overexpression lines showed the opposite results. All above indicate that the *paghyprp1* mutant lines had improved drought and salt tolerance by reducing ROS accumulation, promoting root growth and maintaining root ion homeostasis. 【**Conclusion**】*PagHyPRP1* was confirmed as a negative regulator of the salt and drought stress response in poplar, and the *paghyprp1* mutant lines had improved drought and salt tolerance by reducing ROS accumulation, promoting root growth and maintaining root ion homeostasis. This study provides candidate genes with important breeding value for forest tree stress resistance gene editing and provides empirical evidence and technical reference for the application of CRISPR/Cas9 system to create new germplasm for breakthrough stress resistance in forest trees.

Keywords: CRISPR/Cas9, poplar, *HyPRP1*, salt stress, drought stress, ROS, ion flux

Salt and drought stress are critical environment threats to plant growth and development (Wang *et al.*, 2022; Zhao *et al.*, 2021). Plants have limited potentially available water resources and will face more severe drought and high salinity stress as global climate trends shift toward drought and warming (Chen et al., 2021; Gong et al., 2020). Improving plant salinity and drought tolerance is an effective long-term response to these stresses (Li et al., 2012). It is difficult to improve stress-resistant traits by conventional means, such as hybridization (Pak et al., 2022). Therefore, the creation of new varieties of plants that can tolerate or resist environmental stresses using biotechnology means, such as gene editing, has become a research focus.

The clustered regularly interspaced short palindromic repeats (CRISPR)/CRISPR associated protein 9 (Cas9) system, which can edit a target nucleic acid accurately, has developed rapidly in plant research (Chen *et al.,* 2019; Hua *et al.,* 2019). This system only requires a single guide RNA (sgRNA) with 20 bp to guide Cas9 protein to cleave the target nucleotide sequences accurately (Cong *et al.*, 2013; Ramirez *et al*., 2021). It has the advantages of high editing efficiency, strong specificity and versatility (Chen *et al*., 2019; Ming *et al*., 2022). The CRISPR/Cas9 system has been used for character improvement of rice (*Oryza sativa*), maize (*Zea mays*), wheat (*Triticum aestivum*) and other crops. For example, improved drought and salt tolerance (Shelake, *et al*., 2022), enhanced resistance bacterial blight and *Fusarium wilt* (Zhou, *et al*., 2022; Xu *et al*., 2021). CRISPR/Cas9-mediated maize *ZmESBL* mutant lines significantly increased the Na^+ transmembrane transport capacity and increased the Na^+ transport capacity from roots to shoot through transpiration, thus improving salt tolerance (Wang *et al*., 2022). CRISPR/Cas9 modification of the *ARGOS8* promoter, a negative regulator of maize ethylene response, significantly increased the yield of maize mutants under drought stress (Shi *et al*., 2017). CRISPR/Cas9-mediated knockout of the abscisic acid 8'-hydroxylase (*ABAox*) gene in maize enhanced drought resistance by closing stomata and reducing leaf water loss (Liu *et al*., 2020). The CRISPR/cas9 system mediated two response modulators of rice *OsRR9* and *OsRR10* concurrently to

Funding: This research was supported by the National Key R&D Program of China during the 14th Five-year Plan P eriod (2021YFD2200102), the Basic Research Fund of RIF (Grant No. CAFYBB2020SZ002) and the National Major Proje ct of GMO New Species Cultivation (Grant No. 2018ZX08020002).

***Corresponding author**: Changjun Ding, E-mail: changjunding@caf.ac.cn; Xiaohua Su, E-mail: suxh@caf.ac.cn

# These authors contribute equally.

maintain the balance of Na^+/K^+ ions by regulating the transcription of ion transporters in roots and shoots, thereby improving salt tolerance (Wang *et al*., 2019).

Although CRISPR/Cas9 technology has developed rapidly in model plants and crops, it has made slow progress in woody plants, especially trees. This is mainly due to the characteristics of forest trees, such as their large genome, high heterozygosity, polyploidy and abundant single nucleotide polymorphisms, coupled with a lack of efficient regeneration and genetic transformation systems and other technical difficulties (Pak *et al.*, 2022). To date, the application of CRISPR/Cas9 technology in woody plants has mainly focused on disease resistance, growth and other traits. The CRISPR/Cas9 system was used to mutate the promoter region or coding region of the canker susceptibility gene *CsLOB1* in *Citrus sinensis Osbeck* to obtain citrus cultivars with enhanced resistance to canker disease (Peng *et al*., 2017; Jia *et al*., 2017; Jia *et al*., 2020); CRISPR/Cas9 mediates *VvCCD8* (*carotenoid cleavage dioxygenase 8*) and *VvWRKY52* gene knockdown in *Vitis vinifera* resulted in increased plant outgrowth and gray mycosis resistance, which improved grape yield (Ren *et al*., 2020; Wang *et al*., 2018). Targeted editing of the *MdDIPM4* (DspA/E-interacting proteins of *Malus domestica* 4) gene using the CRISPR/Cas9 system in apple (*Malus domestica*) reduced susceptibility to fire blight (Pompili *et al.*, 2020).

There are a few reports in perennial forests, with most studies focusing on functional verification. CRISPR/Cas9-mediated *LEAFY* mutation in *Eucalyptus grandis* × *urophylla* resulted in uncertain floral development and loss of male and female gametes (Elorriaga *et al*., 2021). The *SAP* gene of male poplar strains (353-FT, *Populus tremula* × *tremuloides*) and female poplar strains (717-FT, *Populus tremula* × *alba*) was knocked out to obtain a completely reproductively sterile line (Azeez *et al*., 2021). However, the effect of its application needs further field observation. Genes related to wood formation were identified using CRISPR/Cas9 technology for cellulase synthase (*PtrCesA*), atypical aspartate protease (*PtAP66*), *PtoMYB156*, *PtoMYB170*, *CSE1* and *CSE2* (Cao et al. 2021; de Vries et al. 2021; Nayeri et al. 2022; Xu et al. 2021; Xu et al. 2017; Yang et al. 2017), The CRISPR/Cas9 system was used to identify biostress-related genes such as transcription factors *MYB115*, *PtrWRKY18* and *PtrWRKY35*, histamine *H3K9* demethylase (*JMJ25*) and salicylate benzoate-glycotransferase (*UGT71L1*) (Fellenberg *et al.,* 2020; Fan *et al.,* 2018; Jiang *et al.,* 2017; Wang *et al.,* 2017b), as well as drought stress response genes of *PtrABRE1*, *PdNF-YB21*, *PtoMYB170* and *PdGNC* (An *et al.,* 2020; Li *et al.,* 2019; Xu *et al.,* 2017; Zhou *et al.,* 2020). In terms of character improvement, CRISPR/Cas9 technology was used to knockout the sequence encoding the P-CR domain binding site of the *PalCESA4* subunit from *Populus alba*, which changed the cell wall structure and improved cellulose production and glycation hydrolysis efficiency (Nayeri *et al*., 2022). However, the use of CRISPR/Cas9 system to identify the function of negatively regulated genes and improve the tolerance traits of poplars has not been reported.

Hybrid proline-rich proteins (HyPRPs) are proline and hydroxyproline-rich cell wall structural proteins (Ma *et al*., 2020b). They comprise a hydrophobic signal peptide, an N-terminal repetitive proline-rich domain, and a conserved C-terminal domain of eight cysteine motifs (8CM), belonging to the CM protein family (Kapoor *et al*., 2019). HyPRPs participate in plant development and in biotic and abiotic stress responses as positive and negative regulators (Banday *et al*., 2022; Debbarma *et al*., 2019; Saikia *et al*., 2020a). Overexpression of rice *OsPRP1*, *Medicago falcata MfHyPRP* and *Cajanus CcHyPRP* significantly increased the tolerance of transgenic plants to drought, salt-alkali, cold and oxidation stress, and blast fungus infection (Nawaz *et al*., 2019; Tan *et al*., 2013; Mellacheruvu *et al*., 2016; Priyanka *et al*., 2010) HyPRPs are also involved in abiotic and biotic stress responses as negative regulators. For example, *SlHyPRP1* (*Solanum lycopersicum*) and *SpHyPRP1* (*S. pennellii*) genes in tomato are negative regulators of multiple abiotic stresses including drought, salt, cold, oxidative stress and ABA. *SlHyPRP1* gene expression was suppressed under various abiotic stresses; however, RNA interference (RNAi) transgenic lines and CRISPR/Cas9-mediated *SlHyPRP1* mutant lines showed enhanced tolerance to oxidative stress, dehydration and salt (Li *et al*., 2016; Saikia *et al*., 2020b; Tran *et al*., 2021). *Gossypium barbadense* silenced for *GbHyPRP1 showed* significantly increased resistance to *V. dahliae* through cell wall thickening and reactive oxygen species (ROS) accumulation (Yang *et al*., 2018a). *Arabidopsis thaliana* heterologously expressing *GhPRP5* became smaller and dwarfed, while RNAi transgenic cotton could regulate the expression of genes related to fiber elongation and wall biosynthesis and increase fiber development (Xu *et al*., 2013). *Capsicum annuum CaHyPRP1* overexpressing plants can negatively regulate basic defense during biological stress by inhibiting ROS scavenging gene expression (Yeom *et al*., 2012).

Although HyPRP proteins have been well characterized in abiotic stress tolerance in various plant species, these plants are mainly cash crops such as tomato, rice, and cotton. In woody plants, only HyPRP protein from *Poncirus trifoliata* has been studied for cold tolerance in leaves by RNAi. However, there have been no reports on HyPRP proteins response mechanism to drought and salt stress in forest trees. 84K poplar (*Populus alba* × *P. glandulosa*) has become a model tree for forest genetic engineering and breeding because of its small genome, relatively complete genome information, strong asexual regeneration ability, and relatively complete genetic transformation system. In the present study, *AtYAO* promoter-driven hspCas9 and the *AtU6* promoter driving two tandem sgRNAs in a CRISPR/Cas9 expression vector were used to target 84K poplar *PagHyPRP1A* and *PagHyPRP1B* genes. *paghyprp1* mutant lines encoding different amino acid sequences with 100% mutation in *PagHyPRP1A* and *PagHyPRP1B* were obtained. Analysis of the mutant lines revealed that the knockout lines of different genotypes could improve drought and salt tolerance by reducing ROS accumulation and maintaining the ion balance in roots, which confirmed that poplar *PagHyPRP1* has a negative regulatory role in salt and drought stress. This study provides candidate genes with important breeding value for forest plant tolerance gene editing, expands the research idea of *HyPRP* gene in woody plants, and provides an empirical and technical reference for the application of the CRISPR/Cas9 system to create new germplasm with breakthrough resistance in forest trees.

1 Materials and methods

1.1 Plant materials and stress treatments

To analyze the expression of the *PagHyPRP1* gene under salt and drought stress, 30-d-old wild-type 84K poplar seedlings grown on 1/2MS solid medium were treated in a hydroponic solution of 200 mM NaCl and 20% PEG-6000 for salt and drought stress, respectively. At the same time, fresh hydroponic solution was used as a control. Leaf, stem and root tissues from three individuals were collected at 0, 3, 6, 12, 24 and 36 h after treatment, and frozen immediately in liquid nitrogen and stored at –80 °C for expression analyses. The experiments were repeated three times.

1.2 Sequence Conservation and Phylogenetic Analysis

The amino acid sequences of HyPRP from different species were retrieved from the National Center for Biotechnology Information (NCBI) database, and the HyPRP sequences of *S. lycopersicum*, *Nicotiana benthamiana*, *Capsicum annuum* and other species were aligned using Clustal X (Thompson et al., 1997). Phylogenetic tree analysis of PagHyPRP1A, PagHyPRP1B, and other HyPRP proteins of known function from different plant species were constructed using MEGA 5.0 based on the neighbor-joining method (Tamura et al., 2011).

1.3 RNA extraction and reverse transcription quantitative PCR (RT-qPCR) analysis

Total RNA was extracted using a RNAprep Pure Plant Plus Kit (TIANGEN BIOTECH, Beijing, China). Then, 1 μg of total RNA was reverse transcribed to cDNA using PrimeScript™ RT Master Mix (Takara, Dalian, China). The qPCR step of the RT-qPCR protocol was performed using the LightCycler® 480 (Roche Applied Science, Penzberg, Germany) real-time quantitative PCR system, and the reaction system and procedure used the TB Green Premix Ex Taq™ kit (Takara). Actinwas used as the internal reference gene, and each sample analyzed separately three times. Relative gene expression was calculated using the $2^{-\triangle\triangle Ct}$ method (Livak and Schmittgen, 2001). All primer sequences used are shown in Table S1.

1.4 Construction of CRISPR/Cas9 expression vector and overexpression vector

To construct a CRISPR/Cas9 expression vector targeting *PagHyPRP1A* and *PagHyPRP1B*, we used the Cas-designer of CRISPR RGEN Tools (http://www.rgenome.net/cas-designer/) to design and screen gRNAs. We then used the Cas-offinder of CRISPR RGEN Tools (http://www.rgenome.net/cas-offinder/) to find potential off-target sites. We selected an sgRNA with a high out-of-frame score, good specificity, no potential off-target sites, and close to the 5' end of the gene coding sequence (CDS) to induce frameshift mutations at the target site, which would result in a loss of gene function. GCAG and AAAC were added to the 5' end of the forward sgRNA1 and reverse sgRNA2 and were included in the PCR forward and reverse primers, respectively. A scaffold and pre-tRNA fragment was using the PUC57 plasmid as a template. The purified PCR fragment and plasmid pHZM58 were digested by *Bsa*I and ligated using T4 ligase according to the Golden Gate reaction method of Qijun Chen from China Agricultural University (Xing et al., 2014) to obtain the CRISPR/Cas9 expression vector phZM58-*pagHyPRP1*. Then, the correctly sequenced plasmid phZM58-*pagHyPRP1* was transferred into Agrobacterium strain GV3101 for subsequent plant infection. pHZM58-*PagHyPRP1* was constructed by Zanmin Hu from the Institute of Genetic Development, Chinese Academy of Sciences.

PagHyPRP1A and *PagHyPRP1B* are 92% similar; therefore, we inserted the CDS of one of the genes, *PagHyPRP1A*, into the 35S-driven pROKII binary vector to obtain the overexpression vector pROKII-*PagHyPRP1*. The correctly sequenced pROKII-*PagHyPRP1* and pHZM58-*PagHyPRP1* plasmids were transferred into *Agrobacterium strain* GV3101 for subsequent plant infestation. All primer sequences used are shown in Table S1.

1.5 Acquisition and identification of *paghyprp1* mutant lines and *PagHyPRP1* overexpressing lines

Genetic transformation of 84K poplar was achieved using the Agrobacterium-mediated leaf disc method (Wang et al., 2016). Resistant buds were screened on MS differentiation medium supplemented with kanamycin (50 mg/L), and resistant plants were screened on 1/2 MS rooting medium supplemented with kanamycin (50 mg/L). Genomic DNA was extracted from the WT and resistant plants using a Hi-Dnasecure Plant Kit (TIANGEN BIOTECH, Beijing, China).

Positive plants containing CRISPR/Cas9 expression vector were screened using *U6*, *Cas9* and *Kan* specific primers in the pHZM58 vector. Furthermore, the full length gene sequences of *PagHyPRP1A* and *PagHyPRP1B* were specifically cloned using the positive plant DNA as a template, respectively. The PCR amplicons were cloned into vector pMD19-T vector (Takara), and 15 positive clones of each amplicon were Sanger sequenced. The mutation type, mutation frequency and genotype were assessed, where mutation frequency was the ratio of the number of mutated clones to the total number of sequenced clones. The overexpression lines (OE) were screened using pROKII vector primers. Their expression levels were verified using RT-qPCR. The details of the primers used are shown in Table S1.

1.6 Analysis of salt and drought tolerance

To examine the growth of tissue culture seedlings under drought and salt stress, terminal shoots of 30-d-old *paghyprp1* mutant lines, OE lines, and WT 84K were rooted in 1/2 MS solid medium supplemented with 1% PEG-6000 and different concentrations of NaCl (0, 50, 75, and 100 mM) for 30 days. Plant growth phenotypes were observed and plant height, root length, whole plant fresh weight, and root fresh weight were determined. Three biological replicates were assessed with six plants per treatment.

To assess salt and drought stress tolerance of soil cultured transgenic plants, *paghyprp1* mutant lines, OE lines and WT grown on 1/2 MS medium for 30 days were transplanted into 12 cm × 12 cm × 15 cm plastic pots containing the same weight of soil and perlite (3:1) mixture. After 45 days of growth in the artificial climate chamber with 16 h light, 25 □ average temperature, and 70–80%

relative humidity, the seedlings at the same growth state were selected for salt and drought simulation stress experiments. About 50 plants of each strain were prepared and divided into three equal portions of about 16 plants each, which were treated with 20% PEG-6000 (drought), 150 mM NaCl (salt) and water (control). There were 3 treatments with 4 block groups and 4 plants in each block group. When collect samples, 1 Plant × 3 blocks = 3 plants were collects of each treatment at each time point. And the other block was used to record the phenotype. The plants were treated with 200 mL of 150 mM NaCl, 20% PEG-6000, and water every 3 d. After 4 days, the root, stem and leaf tissues of PEG-6000 and the control treatment were collected respectively. After 7 days, the root, stem and leaf tissues of PEG-6000, NaCl and control treatment were collected, respectively. After 14 days, the root, stem and leaf tissues of NaCl and control were collected, respectively. After 21 days, above-ground and underground parts of each lines in PEG-6000, NaCl, and normal control were observed and determined. At the same time,roots, stems and leaves were collected separately and incubated in an oven at 80 °C for 72 h to determine the dry weight.

1.7 Histochemical staining and analysis of physiological indices

The 30-d-old *paghyprp1* mutant lines, OE lines and WT tissue culture seedlings were treated with 150 mM NaCl, 10% PEG-6000 and water (control), respectively. After 3 h of stress, the leaves were immersed in NBT and incubated with DAB or Evans blue staining solution. NBT and DAB staining methods were caried out according to Liu *et al*. (2019). Evans blue staining was performed as described by Yang *et al.* (2014).

The contents of O_2^-, H_2O_2, ROS and MDA, the activities of POD and SOD, and the contents of proline in fresh leaves were detected using detection kits from Suzhou Keming Biotechnology Co., LTD. (Suzhou, China).

1.8 Determination of Na^+, K^+, H^+ and Ca^{2+} ion flux in roots and the analysis of gene expression levels related to ion homeostasis

Root ion fluxes were recorded using Non-invasive Micro-test Technology (NMT) (YoungerUSA LLC., Amherst, MA, USA) and iFluxes 1.0 software (YoungerUSA LLC.) (Sun *et al*., 2009a; Xue *et al*., 2020; Ma *et al*., 2020a; Zhang *et al*., 2017; Zhang *et al*., 2019). Na^+, K^+ and H^+ fluxes in the roots of the *paghyprp1* mutant lines, OE lines, and WT were detected under 150 mM NaCl stress for 14 days, and K^+, H^+ and Ca^{2+} fluxes in roots were detected under 20% PEG stress for 7 days. Ion-selective electrodes and calibration solutions were prepared according to previously published descriptions (Ding *et al*. 2020; Zhou *et al*. 2020; Zhao *et al*. 2018; Zhang *et al*. 2015; Sun *et al*). (2009b). The root tips of different lines were taken and equilibrated in the test solution (0.1 mM KCl, 0.1 mM $CaCl_2$, 1.0 mM NaCl, pH 6.0) for 20 min and then continuously measured over 5–10 min to obtain stable Na^+, K^+, H^+ and Ca^{2+} fluxes. Each ion flux of each strain was tested using at least six replicates.

The mRNA expression levels of plasma membrane Na^+/H^+ antiporter (*SOS1*) vacuolar Na^+/H^+ exchanger (*NHX1*) (Pop_G14G045122.T1), Arabidopsis K transporter 1 (*AKT1*) (Pop_A06G079470.T1), plasma membrane H^+ -ATPase (*PMA*) (Pop_G06G035489.T1), calcium-dependent protein kinase 1 (*CPK1*) (Pop_A19G080753.T1) and respiratory burst oxidase homologs (*RBOHF*) (Pop_G03G013842.T1) were analyzed using RT-qPCR with the primers listed in Table S1.

1.9 Statistical analysis

The experimental data were analyzed using one-way analysis of variance (ANOVA) in SPSS (version 22.0; IBM Corp., Armonk, NY, USA). Student's t-test was used to determine the statistical significance between *paghyprp1* mutant lines, OE lines and wild-type 84K. (*, $P < 0.05$; **, $P < 0.01$).

2 Results

2.1 Identification and stress response analysis of *PagHyPRP1* in poplar

In this study, based on the amino acid sequence of SlHyPRP1, a negative regulator of tomato salt and drought, the *PagHyPRP1* gene was obtained in 84K poplar by homologous alignment. *PagHyPRP1* includes two alleles, *PagHyPRP1A* (Pop_A06G061665.T1) and *PagHyPRP1B* (POP_G06G0759191.T1. PagHyPRP1A and PagHyPRP1B encode 198 and 213 amino acids, respectively, with predicted molecular weights of 20.56 kDa and 22.01 kDa. Similar to HyPRPs in other plants, both PagHyPRP1A and PagHyPRP1B proteins contain a signal peptide region, an N-terminal repeated proline-rich region, and a C-terminal 8-cysteine motif (C-C-CC-CXC-C-C-), which belong to the 8CM protein family (Figure S1a). Phylogenetic tree analysis with reported HyPRPs proteins from other plant species showed that PagHyPRP1A and PagHyPRP1B have the highest homology to SlHyPRP1 of *S. lycopersicum* (72.08%, similarity; Figure S1b).

Expression pattern analysis showed that *PagHyPRP1* was mainly highly expressed in the roots, slightly expressed in the leaves, and very low expressed in the stems. (Figure S1c). After salt and drought stress treatments, *PagHyPRP1* expression was significantly inhibited in leaves, stems and roots (Figure S1d, e). The results suggest that *PagHyPRP1* gene might play a negative regulatory role in the poplar salt and drought stress response.

2.2 CRISPR/Cas9-mediated mutations of *PagHyPRP1A* and *PagHyPRP1B* in poplar

To investigate the role of *PagHyPRP1* in salt and drought stress, we targeted alleles *PagHyPRP1A* and *PagHyPRP1B* using the CRISPR/Cas9 system. *PagHyPRP1A* from *P. alba* and *PagHyPRP1B* from *P. tremula var. glandulosa* are located on chromosome chr06 (Figure 1a), and both have only one exon. *PagHyPRP1B* has 45 bp more bases than *PagHyPRP1A* at 225 bp; therefore, two sgRNAs were designed at 57 bp from the start codon of both genes, where sgRNA2 has a 14 bp overlap region with sgRNA1(Figure

1b). The two sgRNAs were constructed into the pHZM58 vector containing hspCas9 driven by the *AtYAO* promoter to obtain a vector containing two tandem pre-tRNA-sgRNA-scaffolds initiated by the *AtU6* promoter (pHZM58-*PagHyPRP1*) (Figure 1c). A total of 75 resistant plants were obtained by screening in medium containing Kanamycin, and 15 positive plants were further tested using vector primers (Figure S2), with a transformation efficiency of 20%.

To investigate the mutations of the two genes in the genome of the positive plants, genomic DNA of 15 positive plants was extracted, *PagHyPRP1A* and *PagHyPRP1B* were specifically amplified, and PCR products and monoclonal were sequenced. The results showed that 9 of the 15 positive plants were mutant plants with mutation efficiency of 60%. Among them, there were two homozygous mutants (#2 and #4) with a 1 bp insertion of T in *PagHyPRP1A* and a 1 bp insertion of C in *PagHyPRP1B*; two allelic mutations (#1 and #3) with a 1 bp insertion of T in *PagHyPRP1A* and a 1 bp insertion of C or A in *PagHyPRP1B*; three chimeric mutants (#5, #6 and #7) with a 1 bp insertion of T or a 1 bp deletion of C in *PagHyPRP1A* and 1 bp or 4 bp deletions in *PagHyPRP1B*; two chimeric mutants (#14 and #15) had multiple mutation types of no change, or 1 bp to 3 bp deletions in *PagHyPRP1A* (Figure 1d, e). And among the 133 sequencing sites of the plasmid clone containing a single amplicon for the *PagHyPRP1A* targets, 128 (96.24%) mutations were detected, including 0 mutations at the Target 1 and 96.24% mutations at the Target 2, of which 79.69% were single nucleotide insertion. Among the 134 sequencing sites of the single amplicon targeting *PagHyPRP1B*, 131 (97.76%) mutations were detected, including 39.55% mutations at the Target 1, all of which were single nucleotide insertion; there were 58.21% mutations at the Target 2, of which 53.73 % were 1 bp to 4 bp deletions (Figure 1e).

The addition or deletion of nucleotides at the target site caused a shift in the protein-coding sequence, resulting in *PagHyPRP1A* and *PagHyPRP1B* knockouts. Among mutant lines #1, #2, #4 and #6, the target sites of the double gene were 100% mutated with different genotypes, and the amino acid sequences encoded by PagHyPRP1A and PagHyPRP1B both contained only the N-terminal signal peptide region (Figure 1f), resulting in the deletion of the structural domain; therefore, these four mutant lines were selected and named *paghyprp1*-#1, *paghyprp1*-#2, *paghyprp1*-#4 and *paghyprp1*-#6 (prp-1, prp-2, prp-4 and prp-6) for subsequent functional studies. In addition, no potential off-target sites were found for either of the two sgRNAs using Case-offinder in CRISPR RGEN Tools. And the target sequence for each gRNA was used for BLASTN searches and was found to contain no single nucleotide polymorphisms (SNPs).

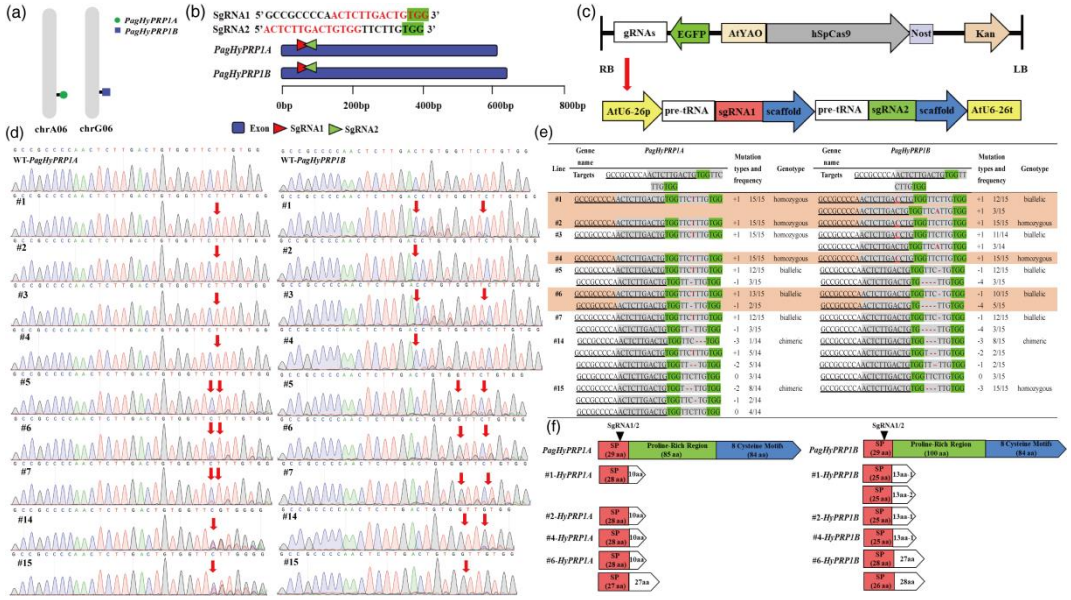

Figure 1 CRISPR/Cas9 expression vector construction and CRISPR/Cas9-mediated mutations of *PagHyPRP1A* and *PagHyPRP1B* in poplar. (a) Relationship between *PagHyPRP1A* and *PagHyPRP1B* on the chromosome. (b) Schematic illustration of the relationship between the positions of the two sgRNAs targeting the coding sequences of *PagHyPRP1A* and *PagHyPRP1B*. The red capital letters are the overlapping regions of the two sgRNAs. (c) Schematic diagram of the CRISPR/Cas9 expression vectors. Two sgRNAs were simultaneously driven by the *Arabidopsis* promoter *AtU6-26p*, which were inserted into the editing vector of *hSpCas9* driven by the *Arabidopsis AtYAO* promoter. (d) The direct sequencing peak map of PCR products containing the target sites of *PagHyPRP1A* and *PagHyPRP1B*. The red arrow indicates the location of the mutations. (e) CRISPR/Cas9-mediated mutation types and mutation frequency statistics of different target sites of *PagHyPRP1A* and *PagHyPRP1B*. The underlined part is the sgRNA1 sequence, the gray shaded part is the sgRNA2 sequence, nucleotide alterations include: --- indicates deletion, red capital letters indicate insertion, + represents addition, - represents deletion, and 0 indicates no alteration. (f) Amino acid sequences of the protein-coding regions deduced from *PagHyPRP1A* and *PagHyPRP1B* in the prp-1, prp-2, prp-4 and prp-6 knockout mutants. CRISPR, clustered regularly interspaced short palindromic repeats; Cas9, CRISPR associated protein 9; sgRNA, single guide RNA; SP, signal peptide.

2.3 Identification of *PagHyPRP1* overexpressing lines and *paghyprp1* mutant lines by RT-qPCR

We obtained 12 *PagHyPRP1* overexpression (OE) lines, which were identified by PCR and reverse transcription quantitative PCR (RT-qPCR) analysis. The differences in *PagHyPRP*1 expression levels among the 12 OE lines were small, at approximately 3.72–6.92 fold higher than in the wild-type (WT) (Figure S3); therefore, OE1 and OE2 lines were randomly selected for further study. Then, the expression levels of *PagHyPRP1* in OE1, OE2 and four *paghyprp1* mutant lines (prp-1, prp-2, prp-4 and prp-6) after salt and drought

stresses were further characterized using RT-qPCR. The results showed that the expression levels of *PagHyPRP1* in both the roots and leaves of OE1 and OE2 lines were significantly higher than those in the WT, and *PagHyPRP1* expression levels in prp-1, prp-2, prp-4 and prp-6 lines were very significantly lower than those in the WT at 7 d or 14 d of normal growth, at 7 d of drought stress, or at 14 d of salt stress (Figure 2), indicating that we successfully obtained *PagHyPRP1* overexpression and knockout lines.

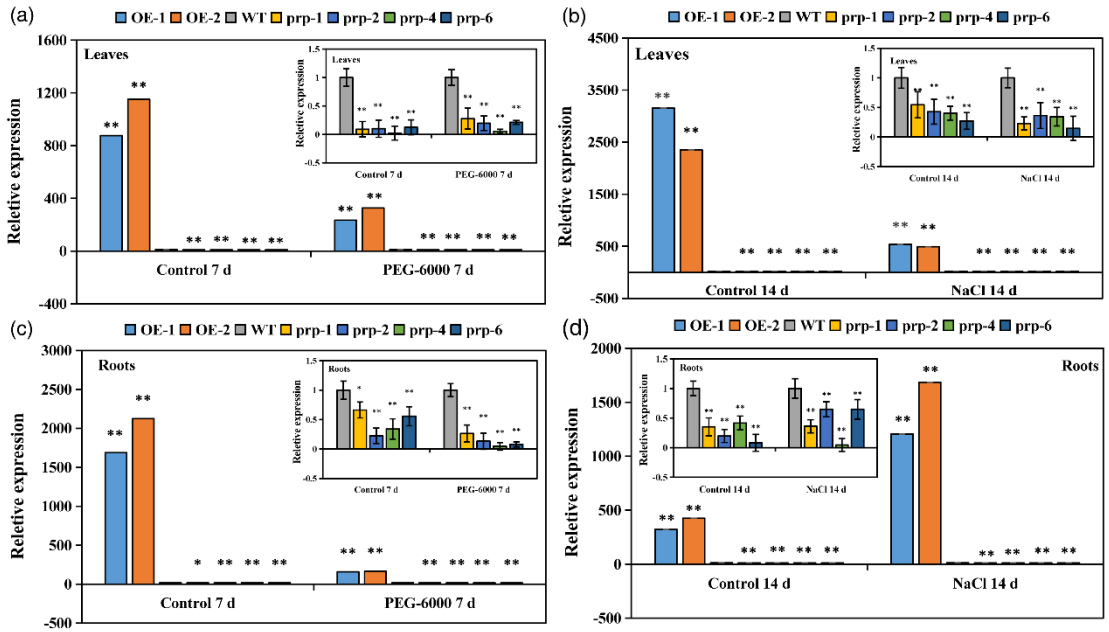

Figure 2 Relative expression levels of PagHyPRP1 in leaves and roots of paghyprp1 mutant lines, OE lines and WT under salt and drought stresses. (a, c) Expression levels of PagHyPRP1 in leaves and roots of paghyprp1 mutant lines, OE lines and WT at normal growth (Control) and 20% polyethylene glycol (PEG)-6000 treatment for 7 d. (b, d) Expression levels of PagHyPRP1 in leaves and roots of paghyprp1 mutant lines, OE lines and WT at normal growth (Control) and 150 mM NaCl treatment for 14 d. Data were processed using the 2-ΔΔCt method. The bars represent the means ± the standard deviation (SD) (n = 3) * indicates significant differences between paghyprp1 mutant lines and OE lines compared with the WT (*P < 0.05; **P < 0.01). OE, overexpression; WT, wild-type.

2.4 The evaluate of tolerance to drought stress of *PagHyPRP1* mutant lines

2.4.1 CRISPR/Cas9 mediated *PagHyPRP1* mutant lines showed better growth under drought and salt stress

To investigate the function of *PagHyPRP1* under drought stress, 3% PEG-6000 was added into normal rooting medium for stress treatment. The results showed that under normal growth conditions (control), there was no significant difference in the growth status of *paghyprp1* mutant lines, OE lines and WT (Figure 3a). After 3% PEG-6000 treatment, the plant height of *paghyprp1* mutant lines was inhibited, but its root length increased obviously. Meanwhile, the plant height, root length, whole plant fresh weight and root fresh weight of *paghyprp1* mutant lines were significantly higher than those of OE lines and WT. In contrast, the OE lines was severely inhibited and almost died (Figure 3a-e). And different lines of tissue culture seedlings were treated with different concentrations of NaCl. The results showed that the growth status of *paghyprp1* mutant lines, OE lines, and WT were basically the same under normal growth conditions (Figure 3f).

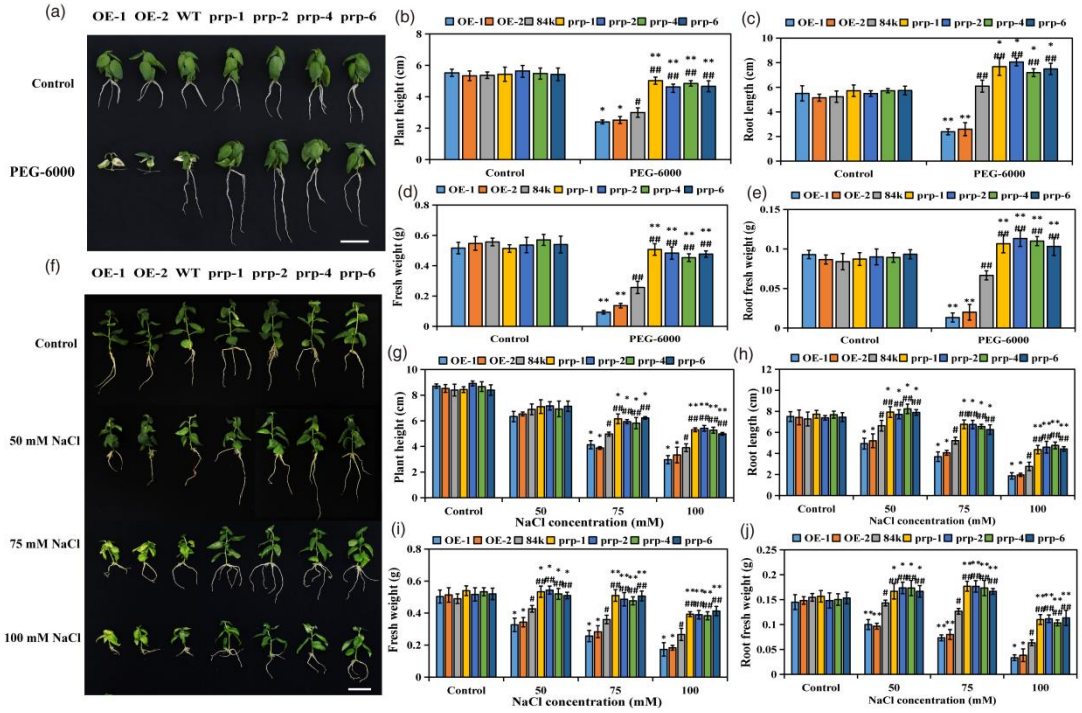

Figure 3 Growth phenotypes of *paghyprp1* mutant lines, OE lines, and WT tissue culture seedlings under drought (a-e) and salt (f-j) stress. Growth phenotypes of 30-d-old *paghyprp1* mutant lines, OE lines, and WT in rooting media containing 1% PEG-6000 (a) and different concentrations of NaCl (0, 50, 75, and 100 mM) (f). Bars indicate 5 cm. (b-e) Plant height, root length, whole plant fresh weight, and root fresh weight of *paghyprp1* mutant lines, OE lines, and WT under 1% PEG-6000 (b-e) and different concentrations of NaCl (g-j). The experiment was repeated three times with two plants each time. The bars represent the means ± the standard deviation (SD) (n = 6), *, ** indicates significant differences between *paghyprp1* mutant lines and OE lines compared with the WT (*$P < 0.05$; **$P < 0.01$). #, ## indicates significant differences between *paghyprp1* mutant lines and WT compared with OE lines (#$P < 0.05$; ##$P < 0.01$). OE, overexpression; WT, wild-type.

2.4.2 CRISPR/Cas9-mediated mutation of *PagHyPRP1* enhances ROS scavenging under drought stress

To further investigate the function of *PagHyPRP1* in response to drought stress under soil conditions, 45-d-old soil seedlings were treated with polyethylene glycol (PEG)-6000. Under normal growth conditions, the growth phenotypes of above-ground and underground parts of *paghyprp1* mutant lines were significantly better than those of OE lines and WT. The stem dry weight and root dry weight of *paghyprp1* mutant lines were significantly higher than those of OE lines and WT, and there was no significant difference between OE lines and WT (Figure 4a). After 21 d of PEG-6000 treatment, the middle and upper leaves of the *paghyprp1* mutant lines maintained normal growth, while only the top leaves of WT plants remained, and OE lines were the most severely damaged, with only the wilted terminal bud portion remaining (Figure 4b). The root growth of all lines was also inhibited, among which the *paghyprp1* mutant lines showed the least inhibition, and their plant height, stem diameter, stem dry weight, root dry weight, and root-shoot ratio were significantly higher (by 1.11–1.46 times) than those of the WT plants. The OE lines showed the opposite result, with parameters being only 0.57 to 0.89 times those of the WT (Figure 4d-h). We next measured the SOD and POD activities and proline contents of all lines. The results showed that the *paghyprp1* mutant lines, OE lines and WT had similar SOD and POD activities and proline contents under control growth conditions (4 d and 7 d). After drought stress (4 d and 7 d), the proline content, and POD and SOD activities of all lines increased, among which the *paghyprp1* mutant lines increased the most, and their proline content, and POD and SOD activities were significantly higher (by 1.12–1.43 times) than in the WT plants. By contrast, these values in the OE lines were only 71.96–86.64% of those in the WT (Figure 4i-k), indicating that the *paghyprp1* mutant lines were able to improve drought tolerance by increasing the proline content, maintaining the osmotic balance, increasing the activities of antioxidant enzymes such as POD and SOD, and reducing the degree of oxidation.

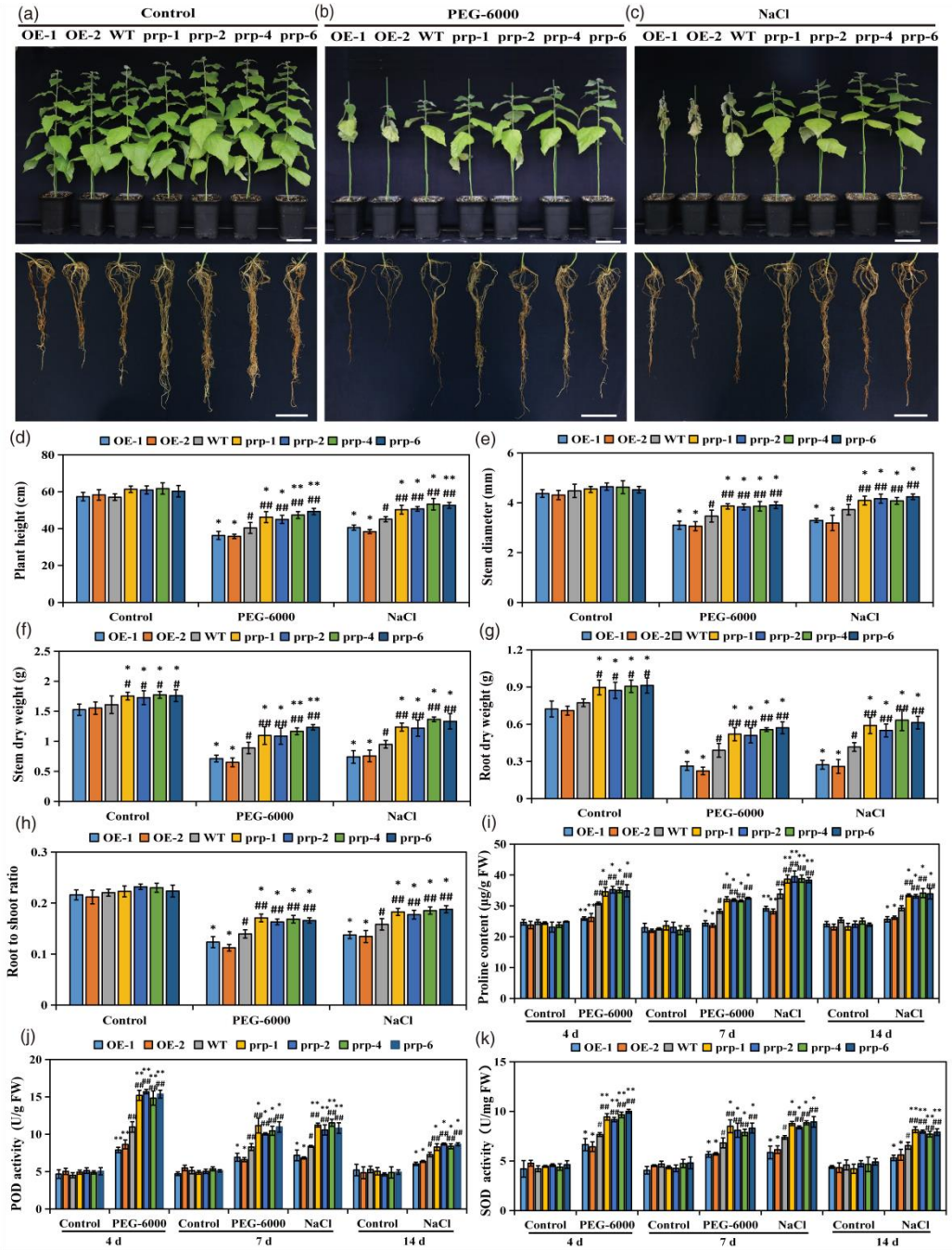

Figure 4 Morphological characteristics of *paghyprp1* mutant lines, OE lines and WT soil-cultured seedlings under drought and salt stress. (a-c) Morphological traits of *paghyprp1* mutant lines, OE lines and WT plants. Bars represent 10 cm. (d-h) Plant height, stem diameter, stem dry weight, root dry weight and root-shoot ratio of *paghyprp1* mutant lines, OE lines and the WT. (i-k) Proline content, and POD and SOD activities of *paghyprp1* mutant lines, OE lines and the WT. 30-d-old *paghyprp1* mutant lines, OE lines and WT tissue culture seedlings were grown in soil for 45 d and irrigated with 0 (control) , 20% polyethylene glycol (PEG)-6000 (drought treatment) every 3 d for 4 d and 7 d , or 150 mM NaCl (salt treatment) every 3 d for 7 and 14 d to determine proline content, and POD and SOD activities. After irrigation for 21 days, the phenotypes of *paghyprp1* mutant lines, OE lines and the WT were observed and plant height and stem diameter, stem dry weight, root dry weight and root-shoot ratio were measured. The bars represent the means ± the standard deviation (SD) (n = 3), *, ** indicates significant differences between *paghyprp1* mutant lines and OE lines compared with the WT (*$P < 0.05$; **$P < 0.01$). #, ## indicates significant differences between *paghyprp1* mutant lines and WT compared with OE lines (#$P < 0.05$; ##$P < 0.01$). OE, overexpression; WT, wild-type.

2.4.3 CRISPR/Cas9-mediated mutations of *PagHyPRP1* reduces oxidative damage under drought stress

To further explore the function of *PagHyPRP1* under drought stress, we compared the biochemical staining of *paghyprp1* mutant lines, OE lines and the WT, in which Nitroblue tetrazolium (NBT) and 3,3′-Diaminobenzidine (DAB) *in situ* staining were performed to detect $O_2^{\cdot-}$ and H_2O_2 accumulation, respectively. Evans blue *in situ* staining was used to detect cell death (Liu *et al.*, 2021b). All lines showed light staining normal conditions, indicating that they had low accumulation of H_2O_2 and $O_2^{\cdot-}$ as well as low levels of cell

damage (Figure 5a). Under drought stress, the staining intensity of each poplar genotype deepened, among which the *paghyprp1* mutant lines had the lowest staining intensity and the lightest color, followed by WT plants, and the OE lines had the deepest color, indicating that the accumulation of H_2O_2 and O_2^- and cell death in *paghyprp1* mutant lines were markedly lower than that in the WT plants and OE lines (Figure 5a). Next, we further determined the contents of O_2^-, H_2O_2, ROS and malondialdehyde (MDA) in fresh leaves after 4 d and 7 d of drought stress. Among them, $O_2^-$and H_2O_2 are important components of ROS (Wang *et al*., 2017a), and MDA represents the degree of lipid peroxidation (He *et al*., 2018). The results showed that under control conditions (4 d and 7 d), the *paghyprp1* mutant lines and OE lines had similar O_2^-, H_2O_2, ROS and MDA contents to the WT. After drought stress treatment, the O_2^-, H_2O_2, ROS and MDA contents of all lines increased. Moreover, the contents of all lines at 7 d were higher than those at 4 d, indicating that with the prolongation of stress, ROS accumulation and the degree of lipid peroxidation increased in all lines. However, the contents of O_2^-, H_2O_2, ROS and MDA in the *paghyprp1* mutant lines were significantly lower than those in the WT plants, at only 0.72–0.86 of the WT level, while the OE lines had significantly higher contents than the WT plants, at 1.09–1.44 times that of the WT, which was consistent with the staining results (Figure 5b-e). These results indicated that the *paghyprp1* mutant lines developed increase drought tolerance by decreasing ROS accumulation, membrane oxidation and cell death.

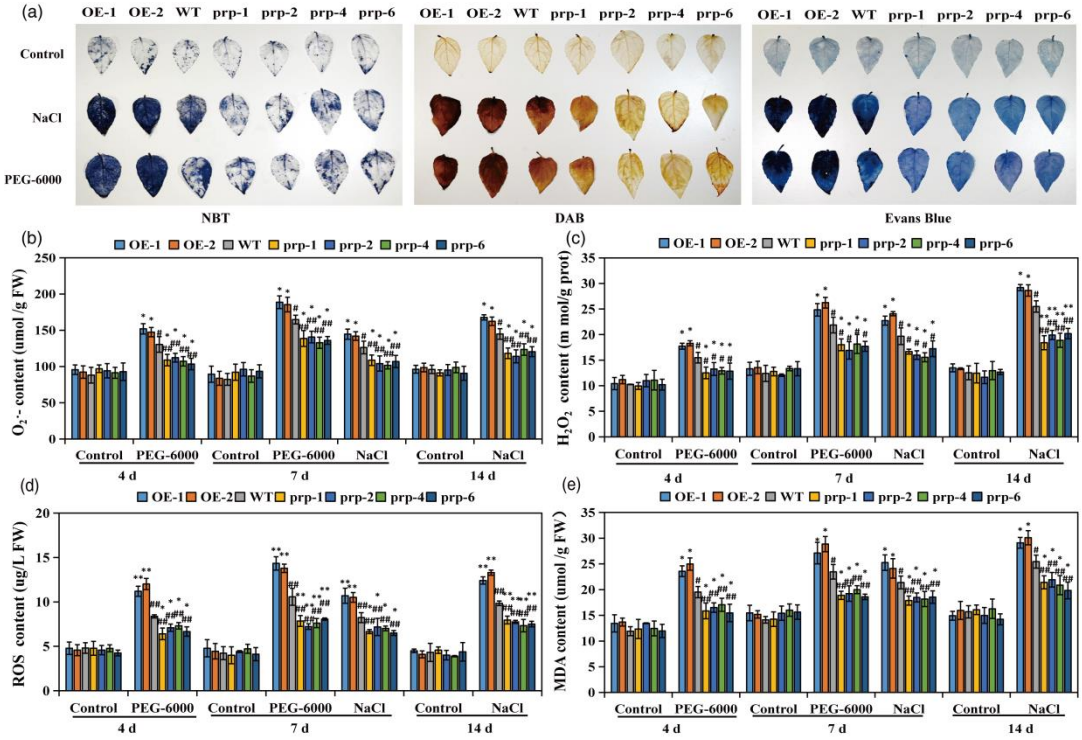

Figure 5 CRISPR/cas9-mediated mutations of *PagHyPRP1* reduces oxidative damage in drought and salt stress. (a) NBT and DAB staining of *paghyprp1* mutant lines, OE lines and WT reveal the accumulation of O_2^- and H_2O_2, and Evans blue staining analysis of cell death. (b-e) The contents of O_2^- H_2O_2, ROS and MDA in *paghyprp1* mutant lines, OE lines and WT. 30-d-old *paghyprp1* mutant lines, OE lines and WT tissue culture seedlings were treated in 10% polyethylene glycol (PEG)-6000 or 150 mM NaCl solution for 3 h and stained with NBT, DAB and Evans blue, with water treatment as a control. 30-d-old 84K *paghyprp1* mutant lines, OE lines and WT of tissue culture seedlings were grown in soil for 45 d and irrigated with 0 (control), 20% PEG-6000 (drought treatment) every 3 d for 4 d and 7 d ,or 150 mM NaCl (salt treatment) every 3 d for 7 d and 14 d. The O_2^-, H_2O_2, ROS and MDA contents were determined. The bars represent the means ± the standard deviation (SD) (n = 3), *, ** indicates significant differences between *paghyprp1* mutant lines and OE lines compared with the WT (*$P < 0.05$; **$P < 0.01$). #, ## indicates significant differences between *paghyprp1* mutant lines and WT compared with OE lines (#$P < 0.05$; ##$P < 0.01$). CRISPR, clustered regularly interspaced short palindromic repeats; Cas9, CRISPR associated protein 9; OE, overexpression; WT, wild-type; NBT, Nitroblue tetrazolium; DAB, 3,3′ -Diaminobenzidine; ROS, reactive oxygen species; MDA, malondialdehyde.

2.4.4 CRISPR/ Cas9-mediated mutation of *PagHyPRP1* regulates Ca^{2+}, K^+ and H^+ ion flux under drought stress

To investigate whether *PagHyPRP1* is involved in the regulation of ion balance, we measured Ca^{2+}, K^+ and H^+ ion flux (600 μm from the root tip) of the *paghyprp1* mutant lines, OE lines and WT plants using Non-invasive Micro-test Technology (NMT) after 7 d of drought stress treatment. Under normal growth conditions, all lines had low Ca^{2+} and H^+ influx, and K^+ efflux. After drought stress, the *paghyprp1* mutant lines displayed a much higher (by 1.20–1.39 times) Ca^{2+} influx than that of WT; while the Ca^{2+} influx in the OE lines was significantly lower (by 0.68 and 0.74 times) than that in the WT (Figure 6a). Drought stress also increased the H^+ influx, and the *paghyprp1* mutant lines showed higher (by 1.27–1.43 times) H^+ influx than that in the WT; while the OE lines exhibited a significantly lower (66.48–71.39%) H^+ influx than that in the WT (Figure 6c). Meanwhile, drought stress caused K^+ efflux, and the *paghyprp1* mutant lines had a lower (by 0.60–0.72 times) K^+ efflux compared with that in the WT; while the OE lines had a more pronounced (by 21.83% and 29.28%) K^+ efflux than that in the WT (Figure 6b). In addition, we compared the expression levels of some key genes affecting plant ion homeostasis in the *paghyprp1* mutant lines, OE lines and WT, such as *CPK1* for Ca^{2+} transport and

signaling; *AKT1* for K^+ uptake and transport; *PMA* that drives ion transport; and *RBOHF*, which encodes NADPH oxidase and is involved in Ca^{2+} signaling under drought stress. Under normal growth conditions, the expression levels of *CPK1*, *AKT1*, *PMA* and *RBOHF* in the *paghyprp1* mutant lines and OE lines were not significantly different from those in the WT (Figure 6d). After drought stress, the expression levels of the four genes were significantly different, among which the expression levels of *CPK1*, *AKT1* and *PMA* in the *paghyprp1* mutant lines were significantly higher, and the expression level of *RBOHF* was significantly lower, than in the WT and the OE lines showed the opposite results (Figure 6e). Taken together, these results suggested that the *paghyprp1* mutant lines might improve drought resistance by regulating the expression of ion homeostasis-related genes to increase Ca^{2+} and H^+ influx, reduce K^+ efflux, and maintain the intracellular ion balance.

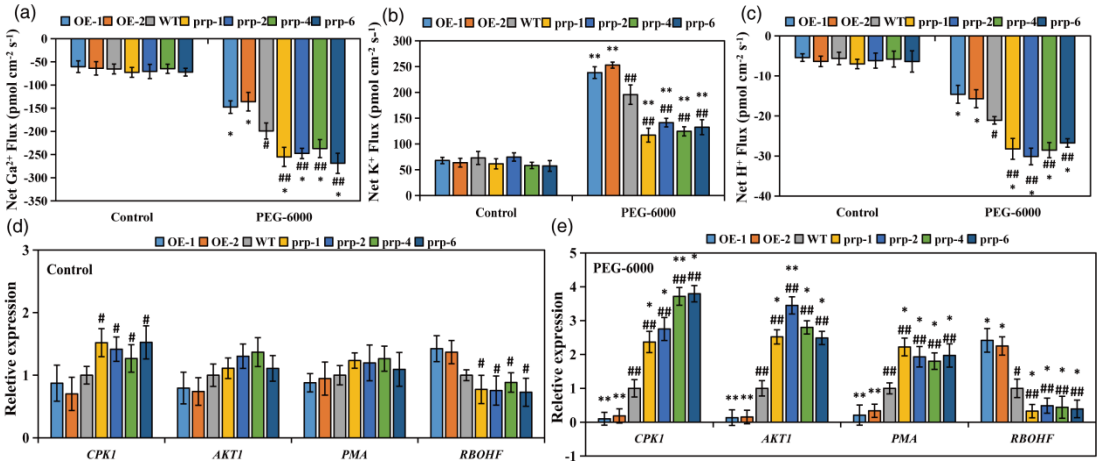

Figure 6 Ca^{2+}, K^+ and H^+ ion flux and ion transport-related gene expression in *paghyprp1* mutant lines, OE lines and WT root tips under drought stress. (a-c) Ca^{2+}, K^+ and H^+ ion flux in root tips. The bars represent the means ± the standard deviation (SD) (n = 6). (d-e) Expression levels of *CPK1*, *AKT1*, *PMA* and *RBOHF* in *paghyprp1* mutant lines, OE lines and the WT. The bars represent the means ± the standard deviation (SD) (n = 3). *, ** indicates significant differences between *paghyprp1* mutant lines and OE lines compared with the WT (*$P < 0.05$; **$P < 0.01$). #, ## indicates significant differences between *paghyprp1* mutant lines and WT compared with OE lines (#$P < 0.05$; ##$P < 0.01$). OE, overexpression; WT, wild-type.

2.5 The evaluate of tolerance to salt stress of *PagHyPRP1* mutant lines

2.5.1 CRISPR/Cas9 mediated *PagHyPRP1* mutant lines showed better growth under salt stress

Under different concentrations of NaCl, the growth of all lines was inhibited. The OE lines were more severely inhibited by increasing salt concentration, in which plant height, root length, whole plant fresh weight, and root fresh weight were significantly lower than those in the WT. The plant heights of the *paghyprp1* mutant lines were reduced, however, the number of primary roots were significantly increased and the root length was less inhibited, making the root fresh weight of the *paghyprp1* mutant lines significantly higher than that of the WT (by 1.29–2.08 times). In addition, the plant height, root length (except 50 mM NaCl) and whole plant fresh weight of the *paghyprp1* mutant lines were significantly higher than those of the WT and OE lines (Figure 3g-j). Indicating that *PagHyPRP1* may play an important role in poplar roots.

2.5.2 CRISPR/Cas9-mediated mutations of *PagHyPRP1* enhances ROS scavenging under salt stress

We further explored the function of *PagHyPRP1* in salt stress in soi. The results showed that after NaCl treatment for 21 d, all the leaves of the OE lines and WT plants were wilted to abscission, whereas the upper half of the *paghyprp1* mutant lines maintained normal growth; however, the lower leaves wilted and withered (Figure 4c). In addition, the root growth of all lines was inhibited; however, the roots of the *paghyprp1* mutant lines were significantly less inhibited than other plants, which resulted in the plant height, stem diameter, stem dry weight, root dry weight and root-shoot ratio of the *paghyprp1* mutant lines being significantly higher (by 1.11–1.52 times) than those of the WT plants. The OE lines showed the opposite result, with these parameters being only 0.62–0.88 times that of the WT (Figure 4d-h). These results were consistent with those of the tissue culture seedlings. Then, we measured the activities of superoxide dismutase (SOD), peroxidase (POD) and the contents of proline in fresh leaves of all lines. Under control growth conditions (7 d and 14 d), there were no significant differences in the contents of proline, SOD and POD between the *paghyprp1* mutant lines and the OE and WT lines. The proline content, and POD and SOD activities of all genotypes increased under salt stress, but the contents at 14 d were lower than those at 7 d, indicating that the POD and SOD activities of all lines decreased gradually with extended stress time. However, the proline content, and POD and SOD activities of the *paghyprp1* mutant lines were significantly higher than those of the WT plants, increasing by 1.13-1.37 times compared with those of WT. Meanwhile, the contents in the OE lines were significantly lower than those in the WT plants at both 7 d and 14 d under salt conditions, at only 79.38–87.37% of the WT contents (Figure 4i-k). These results indicated that the *paghyprp1* mutant lines could improve the salt tolerance of plants by increasing the content of proline, enhancing the activities of antioxidant enzymes such as POD and SOD, and reducing the accumulation of ROS.

2.5.3 CRISPR/Cas9-mediated mutations of *PagHyPRP1* reduces oxidative damage under salt stress

To investigate whether CRISPR/Cas9-mediated *PagHyPRP1* mutation could also reduce the oxidative damage to poplar under salt stress, we performed DAB and NBT staining, and $O_2^{\cdot-}$, H_2O_2 and ROS content determination. The results showed that the leaf color

range of *paghyprp1* mutant lines was the smallest and the color was the lightest after salt stress, followed by the WT and OE lines (Figure 5a). After 7 d and 14 d of PEG-6000 treatment (to simulate salt conditions), the accumulations of $O_2^{\cdot-}$, H_2O_2 and ROS in the *paghyprp1* mutant lines were significantly lower (at 0.72–0.87 times) than those in the WT; whereas in the OE plants, the levels of these factors were significantly higher (by 1.12–1.35 times) than in WT plants (Figure 5b-d). The results of Evans blue staining and MDA content determination showed that the *paghyprp1* mutant lines had the lightest staining, while the OE lines had the deepest staining after salt stress (Figure 5a). After 7 d and 14 d of PEG-6000 treatment, the MDA content of *paghyprp1* mutant lines were significantly lower (by 78.01–86.73%) than in the WT plants. By contrast, the MDA content of the OE lines increased by 1.13–1.18 times comparted with that of the WT (Figure 5e). In conclusion, the *paghyprp1* mutant lines could maintain relatively low $O_2^{\cdot-}$, H_2O_2, ROS and MDA levels after both 7 d and 14 d of salt stress, indicating that *paghyprp1* lines could improve salt resistance by maintaining low oxidative damage, reducing cell death, and protecting cell membrane integrity.

2.5.4 CRISPR/Cas9-mediated mutations of *PagHyPRP1* regulates Na^+, K^+ and H^+ ion flux under salt stress

To better understand the function of *PagHyPRP1*, we measured the Na^+, K^+ and H^+ ion flux and related gene expression levels in the *paghyprp1* mutant lines, OE lines and WT plants (600 μm from the root tip) after 14 d of salt stress treatment. The results showed that under normal growth conditions, all lines exhibited Na^+ and K^+ efflux, and the efflux levels of the different lines were similar (Figure 7a, b). After salt stress, Na^+ efflux increased significantly in all lines. Notably, the *paghyprp1* mutant lines showed higher (by 1.32–1.66 times) Na^+ efflux than the WT. However, the Na^+ efflux in the OE lines was significantly lower (only 0.60 and 0.69 times) than that of the WT (Figure 7a). Salt stress also increased the K^+ efflux in all lines, with the *paghyprp1* mutant lines displaying a much lower (by 0.63–0.78 times) K^+ efflux than the WT; the OE lines showed a significantly higher (0.26 and 0.35 time) K^+ efflux than that of the WT (Figure 7b). The H^+ influx was weak (0 pmol cm^{-2} s^{-1}) in all lines under normal conditions and increased significantly after salt stress. The H^+ influx in *paghyprp1* mutant lines was much higher (by1.45–1.70 times) than that in the WT. However, the OE lines showed lower H^+ influx (by 0.46 and 0.55 times) than the WT (Figure 7c). Under control conditions, the expression levels of only two genes, *NHX1* and *PMA*, in the *paghyprp1* mutant lines were significantly higher than those in the WT, and the OE lines showed the opposite results (Figure 7d). Under salt stress, the expression levels of the five genes were significantly different. Among them, the expression levels of *SOS1*, *NHX1*, *AKT1* and *PMA* in the *paghyprp1* mutant lines were significantly higher than those in the WT, while *RBOHF* expression was significantly lower than that in the WT. The opposite results were observed in the OE lines (Figure 7e). These results suggested that the *paghyprp1* mutant lines might increase Na^+ efflux and H^+ efflux and decrease K^+ efflux by regulating the expression of genes related to ion homeostasis, thereby maintaining intracellular Na^+/K^+ homeostasis and improving plant salt tolerance.

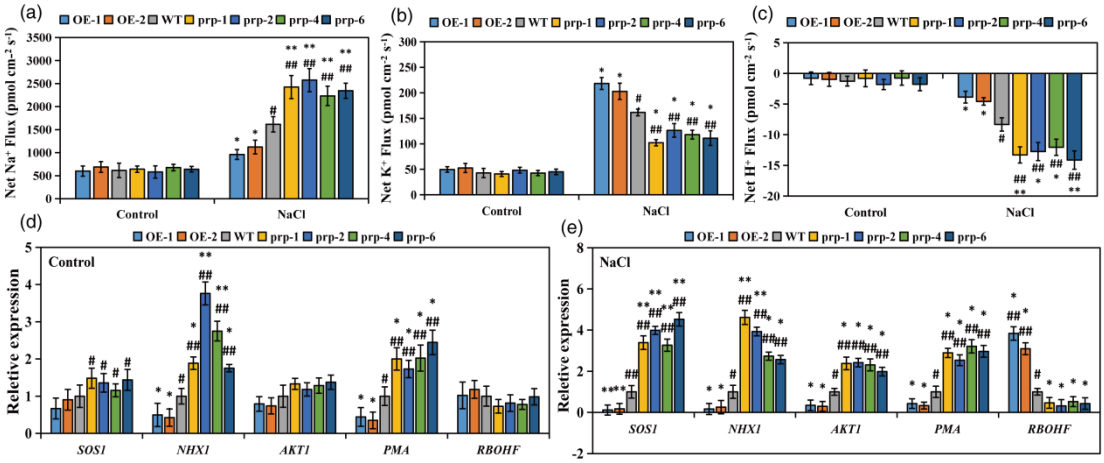

Figure 7 Na^+, K^+ and H^+ ion flux and ion transport-related gene expression in *paghyprp1* mutant lines, OE lines and WT root tips under salt stress. (a-c) Na^+, K^+ and H^+ influx in root tips. Positive values indicate efflux, negative values indicate inflow. The bars represent the means ± the standard deviation (SD) (n = 6). (d-e) Expression levels of *SOS1*, *NHX1*, *AKT1*, *PMA* and *RBOHF* in *paghyprp1* mutant lines, OE lines and the WT. The bars represent the means ± the standard deviation (SD) (n = 3). *, ** indicates significant differences between *paghyprp1* mutant lines and OE lines compared with the WT (*P < 0.05; **P < 0.01). #, ## indicates significant differences between *paghyprp1* mutant lines and WT compared with OE lines (#P < 0.05; ##P < 0.01). OE, overexpression; WT, wild-type.

3 Discussion

3.1 Identification of *PagHyPRP1* gene function in poplar

Previous studies have shown that most HyPRPs could act as positive and negative regulators of biotic and abiotic stress in plants (Banday *et al.*, 2022). However, there are few studies on the involvement of poplar *HyPRPs* in responses to abiotic stress. *HyPRPs* are conserved and show diverse distribution, exerting different roles in the responses of different plants to biotic and abiotic stresses (Saikia *et al.*, 2020a). The studies of HyPRP proteins participating in abiotic stress response in the reported plants were mainly focused on leaves. For example, *SlHyPRP1* was mainly expressed in the leaves of *S. lycopersicum* (Li *et al.*, 2016). And in *P. trifoliata*, *PtrPRP* was expressed in both roots, stems and leaves (Peng *et al.*, 2015). In this study, *PagHyPRP1* gene was mainly highly expressed in the roots, slightly expressed in the leaves, and very low expressed in the stems (Figure S1). This is different from the expression of *HyPRP*

genes in reported plants, indicating that the regulatory mechanisms of *PagHyPRP1* may be different. Salt and drought stress experiments under medium and soil conditions showed that the *pagHyPRP1* mutant lines had better growth phenotypes than the WT and OE lines. The root system of the *paghyprp1* mutant lines were the most developed, with significantly higher root length and root weight (fresh and dry weight) than WT and extremely significantly higher than OE lines (Figure 3, 4), indicating that the root system of the *paghyprp1* mutant lines may play an important role in drought and salt stress. At the same time, in soil seedlings, the growth phenotype of the above-ground and underground parts of *paghyprp1* mutant lines were significantly better than OE lines and WT plants under normal growth conditions, which was different from previous studies on *SlHyPRP1*, which did not cause significant developmental phenotype changes under no stress conditions (Li *et al*., 2016), indicating that the absence of *PagHyPRP1* gene may also promote the growth of poplar under non-stress conditions. The above results showed that *paghyprp1* mutant lines had better growth phenotype, more developed root system and higher stress tolerance, suggesting that *PagHyPRP1* might act as a negative regulator in poplar salt and drought stress response, in which root system may play an important role.

3.2 CRISPR/Cas9-mediated mutations of *PagHyPRP1* reduce oxidative damage under salt and drought stress in poplar

Under normal growth conditions, plants maintain redox homeostasis through self-regulation, and when exposed to adverse environments, a large amount of ROS will accumulate, resulting in oxidative damage (Wang *et al*., 2021; Li *et al*., 2022; Zhou *et al*., 2020); therefore, scavenging of ROS is important to improve plant stress tolerance. The antioxidant enzymes SOD and POD play important roles in the removal of ROS and can affect the cellular ROS level (Liu *et al*., 2021a). In addition, proline, as an important osmotic regulator, has an important function in preventing stress damage to plants (Zhang *et al*., 2019a). In this study, under salt and drought stress, the *paghyprp1* mutant lines showed higher SOD and POD activities; a higher proline content; and lower O_2^-, H_2O_2, ROS and MDA levels than the WT, whereas OE lines exhibited severe ROS-mediated damage (Figure 4, 5). These results suggested that the improved salt and drought tolerance of the *paghyprp1* lines could be attributed to their lower ROS levels and higher proline content. This is similar to the positive or negative regulation mechanisms of *HyPRPs* in other plants. For example, *SlHyPRP1*-RNAi transgenic lines in tomato showed improved oxidative stress tolerance by increasing the expression of ROS scavenging genes such as *SOD*, *CAT* and *MsrB* (Li *et al*., 2016). *PtrPRP*-RNAi plants of trifoliate orange had higher electrolyte leakage and MDA content, increased ROS accumulation, and lower levels of proline than WT plants, and showed higher sensitivity under low temperature stress (Peng *et al*., 2015). CRISPR/Cas9-mediated rice *OsPRP1* mutants had decreased antioxidant enzyme activity and proline, chlorophyll, abscisic acid (ABA) and ascorbic acid (AsA) contents under low temperature stress, resulting in decreased stress resistance (Nawaz *et al*., 2016). CaMV35S-*CcHyPRP* (*Cajanus cajan*) conferred tolerance to salt, drought and heat stress in transgenic rice by enhancing catalase (CAT) and SOD activities and reducing MDA levels (Mellacheruvu *et al*., 2016).

3.3 CRISPR/Cas9-mediated mutations of *PagHyPRP1* improve ion homeostasis and signaling under drought stress in poplar

Calcium ions (Ca^{2+}) are important secondary messengers in signal transduction in response to various stresses in plants (Dong *et al*., 2022; Dodd *et al*., 2010). Drought stress can stimulate a unique Ca^{2+} signal that is received and sensed by Ca^{2+} sensors, such as calcium-dependent protein kinases (CPKs), to elicit a series of physiological and biochemical responses to the adverse environment (Dong *et al*., 2022; Chen *et al*., 2021). K^+ can promote water uptake in plants by regulating the cellular osmotic potential (Sklodowski *et al*., 2017; Boscari *et al*., 2009). Drought stress can activate outward rectifying K^+ channels and lead to cellular K^+ efflux; therefore, it is very important to maintain cellular K^+ homeostasis (Feng *et al*., 2016). Inward-rectifying K^+ channels, such as AKT1, are major contributors to K^+ uptake and transport (Zhao et al., 2021; Very et al., 2003). K^+ uptake by plants is mediated by the electrical gradient and proton motive force provided by H^+-ATP (Shabala *et al*., 2016). K^+, H^+ and Ca^{2+} transport and balance in mesophyll cells are regarded as potential chemical signals and indicators of drought stress in soybean (Mak *et al*., 2014) and barley (Feng *et al*., 2016). In this study, the *paghyprp1* mutant lines showed higher expression of *CPK1*, *AKT1* and *PMA* under drought stress, and maintained higher Ca^{2+} influx and lower K^+ efflux (Figure 6). These results suggested that the *paghyprp1* mutant lines might increase Ca^{2+} influx and decrease K^+ efflux by participating in Ca^{2+} signaling to regulate ion homeostasis and improve plant drought resistance. At the same time, the *paghyprp1* mutant lines showed higher H^+ influx, which might lead to alkalization of apoplasts in the roots. "Extracellular alkalinization" can act as a signal to regulate the process of plant growth and immunity, slow down growth, enhance immunity and enhance environmental adaptability (Liu *et al*., 2022). Previous studies have shown that alkalinization of xylem sap pH is an early response to drought stress in plants (Li *et al*. 2021b; Bahrun *et al*., 2002; Jia and Davies, 2007). Feng *et al.* (2016) and li *et al.* (2021b) found that drought tolerance in barley was associated with high H^+ influx in the leaf mesophyll. In addition, overexpression of *HvAKT2* and *HvHAK1* in barley enhanced plant K^+ uptake and H^+ homeostasis, which in turn improved drought tolerance in transgenic lines (Feng *et al*. 2020). Recently, it was shown that overexpression of *Dendrobium catenatum* DcCIPK24 increased drought and salt tolerance of transgenic *Arabidopsis* by increasing Ca^{2+} and H^+ influx (Zhang *et al*., 2022).

3.4 CRISPR/Cas9-mediated mutations of *PagHyPRP1* improve ion homeostasis under salt stress in poplar

In addition to oxidative damage and osmotic stress, salt stress can also cause ion toxicity (Van *et al*., 2020; Zhang *et al*., 2019b). Under salt stress, excessive sodium uptake by plant cells causes depolarization of the plasma membrane, which in turn activates outward

potassium channels to cause K^+ efflux, resulting in a K^+/Na^+ ratio imbalance (Wu *et al.*, 2018; Sun *et al.*, 2018). SOS channels play an important role in maintaining ion homeostasis in plant cells (Zhu *et al.*, 2016; Yang *et al.*, 2018b; Mahi *et al.*, 2019). The Na^+/H^+ antiporter (SOS1) located at the plasma membrane is responsible for transporting excess Na^+ from the cytoplasm to the extracellular space (Shi *et al.*, 2000; Yin *et al.*, 2020b), and the vacuolar localized Na^+/H^+ antiporter (NHX1) can mediate vacuolar Na^+ compartmentalization and catalyze the electroneutral exchange of H^+ for Na^+ or K^+ (Barragan *et al.*, 2012; Bassil *et al.*, 2019). Intracellular retention of K^+ helps to withstand stress from Na^+ shock. During salt stress, K^+ can be transported into cells through *AKT1* to maintain a high K^+/Na^+ ratio (Zhang *et al.*, 2019b; Ali *et al.*, 2019). The plasma membrane H^+-ATPase (PMA) can maintain the cellular H^+ gradient and provide the proton motive force required for the Na^+/H^+ reverse transporter (Li *et al.*, 2022; Chen *et al.*, 2021; Bassil *et al.*, 2014); it can also limit Na^+ input and K^+ output by affecting the membrane polarity of the intercellular compartment (Van et al., 2020). In this study, *paghyprp1* mutant lines showed higher expression of *SOS1*, *NHX1*, *AKT1* and *PMA*, higher Na^+ efflux and H^+ efflux, and lower K^+ efflux (Figure 7), indicating that *paghyprp1* mutant lines might increase Na^+ efflux and limit K^+ efflux in the roots by inducing the expression of ion transport-related genes, thereby maintain a high K^+/Na^+ ratio to enhance their salt tolerance. According to Ding *et al.* (2020) and Su *et al.* (2019), higher net Na^+ efflux, H^+ influx, and stronger inhibition of K^+ efflux can effectively improve salt tolerance. For example, higher expression levels of *NHX1* and *SOS1* induced by salt stress in transgenic poplar ABJ01, resulted in increased accumulation of the Na^+/H^+ antiporter, inducing higher net Na^+ efflux, H^+ influx, and lower K^+ efflux to effectively improve salt tolerance; and *Arabidopsis pop2-5* mutants could regulate K^+ retention and Na^+ exclusion by increasing the expression of *SOS1*, *NHX1* and *AHA2* (H^+-ATPase) to improve plant salt tolerance. Moreover, the salt-tolerant model species *Populus euphratica* maintains cell viability under long-term salt stress by upregulating the expression of *SOS1*, *NHXI*, *PMA*, *CPK1* and other genes to increase the influx of H^+, Cl^-, Ca^{2+} and the efflux of Na^+, and reduce K^+ loss under salt stress to maintain ion homeostasis (Zhang *et al.*, 2015).

3.5 CRISPR/ Cas9-mediated *PagHyPRP1* mutant lines are involved in ROS signaling under salt and drought stress

ROS are closely related to the generation and regulation of plant signals in response to biotic or abiotic stress (Gilroy *et al*., 2016). ROS play a dual role in plants. An appropriate amount of ROS can act as signal molecules in response to abiotic stress (Marino *et al*., 2012), while excessive ROS will break the intracellular oxidative balance and cause damage to plants (Gill *et al*., 2010). Studies have shown that NADPH oxidase, encoded by respiratory burst oxidase homologs (*RBOHs*), is the main source of ROS production and accumulation in apoplasmic bodies under stress conditions (Kadota *et al*., 2015). lower expression of *RBOHF* in mutants could modulate appropriate ROS signalling, such as H_2O_2, then activate various Ca^{2+} channels and promote Ca^{2+} influx in extracellular via HPCA1. Under drought-simulated stress, Ca^{2+} signalling could activate *CPK1* and other CPKS to promote Ca^{2+} signal transduction and trigger transcriptional responses to stress. Meanwhile, the higher levels of *CPK1* might, in turn, promote Ca^{2+} influx (Chen *et al.,* 2021; Zhang *et al.,* 2022; Mittler *et al*., 2022). In addition, the increased H^+ influx and decreased K^+ effluxmight result from the upregulation of *PMA* and *AKT*. Higher levels of ion concentration in the mutants could benefit the formation of osmoregulation substances and reduce the intracellular water potential, which then improves the drought tolerance by maintaining the balance of osmotic pressure (Figure 8). Likewise, under salt stress, the appropriate ROS might form a "ROS-Ca^{2+}" hub to activate the SOS signalling pathway (Chen *et al.,* 2021). Hence the upregulated expression of *SOS1* and *NHX1* in the mutants could activate Na^+/H^+ transporters to promote Na^+ efflux and H^+ influx. Besides, the increased levels of *PMA* and *AKT1* expression in the mutants indicated limit levels of K^+ effluxand enhanced electrogenic proton (H^+) pumps, resulting in higher levels of salt tolerance in the mutants by maintaining the balance of Na^+/K^+ in intracellular (Figure 8).

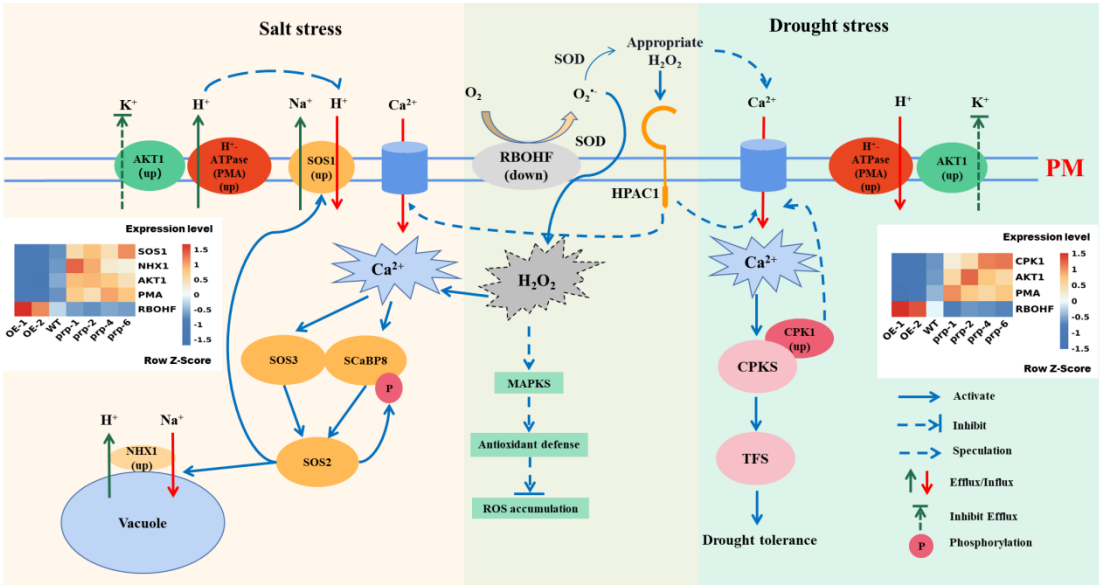

Figure 8 ROS signalling pathway analysis of mutant lines in response to drought and salt stress. The double lines at the top represent the plasma membrane. The light orange and light green backgrounds show signal transduction and ion transport under salt stress and drought stress, respectively. The overlaps are shared by salt and drought stress. The sensors are separated in this image for clarity. The relative expression levels in p were Z-scaled $\log_2$FPKM.

4 Conclusion

This study shows a successful multilocus genome editing on *PagHyPRP1* of *P. alba* × *P. glandulosa* by CRISPR/Cas9, with a 60% editing efficiency. The mutations were stable over the asexual propagation procedure, and the *PagHyPRP1* expression was almost undetectable. The four new mutants were integrated into the poplar germplasms with significantly improved drought and salt tolerance. This work also opens a new avenue for applying CRISPR/Cas9 to create new germplasm for stress resistance in forest trees. This great input to the new poplar germplasms can facilitate forestation in difficult environments.

Supporting Information

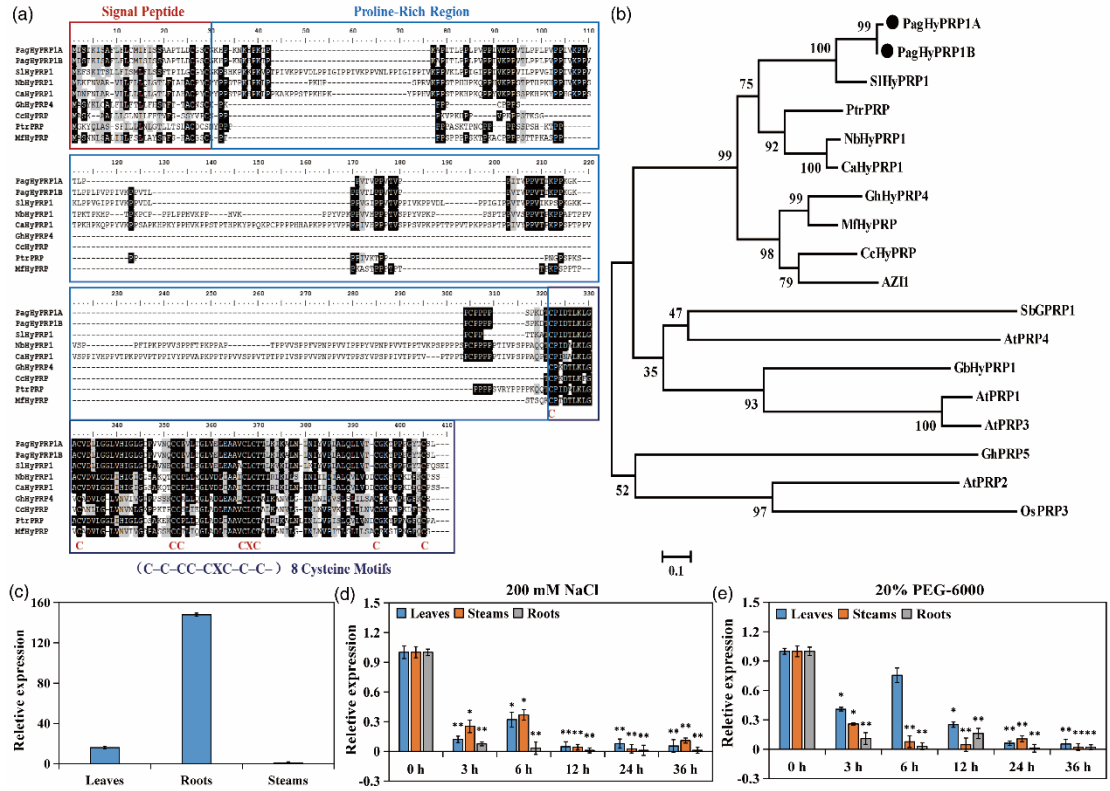

Figure S1 Multiple alignment, phylogenetic analysis, and expression analysis of *PagHyPRP1A* and *PagHyPRP1B*. (a) Sequence alignment of the deduced PagHyPRP1A and PagHyPRP1B sequences with other HyPRP sequences. The signal peptides are framed in red, the proline-rich region are framed in light blue, and the C-terminal eight cysteine motifs are framed in dark blue. Identical amino acids are shaded in black, and similar amino acids are shaded in gray. (b) Phylogenetic tree analysis of PagHyPRP1A, PagHyPRP1B and reported HyPRP proteins from other plant species using the neighbor-joining method in the MEGA v.5.0 software. The scale bar represents 0.1 substitutions per site. (c) Relative expression level of PagHyPRP1 in the leaf, root, and stem. The expression level in the stem was normalized to 1. (d, e) Relative expression levels of *PagHyPRP1* in leaves, roots and stems of poplars under salt and drought stress. 30-d-old wild-type 84K poplar seedlings were subjected to 200 mM NaCl and 20% polyethylene glycol (PEG)-6000 for the indicated times. The bars represent the means ± the standard deviation (SD) (n = 3).

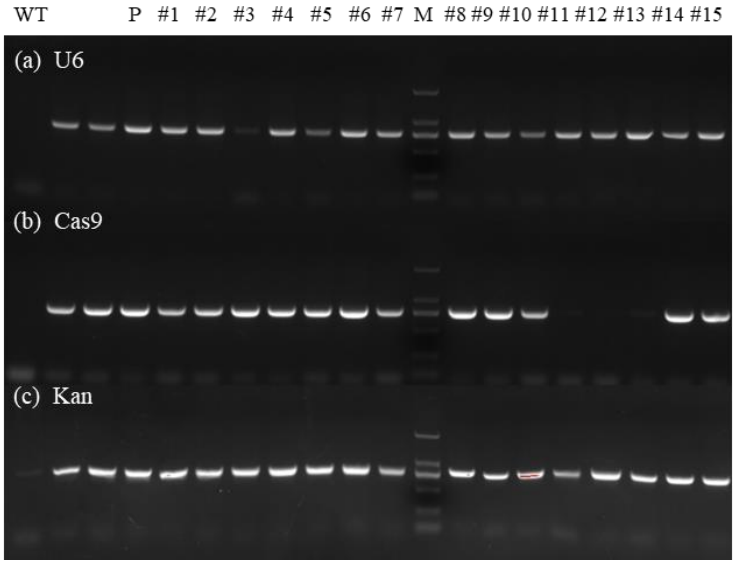

Figure S2 Identification of *paghyprp1* mutant lines by using a genomic DNA PCR analysis of the *U6*, *Cas9* and *Kan*. #1-#15: 15 mutant lines; WT: wild type; P: The plasmid DNA of pHZM58-*PagHyPRP1*cassette binary vector as a positive control; M: 2000 bp DNA markers.

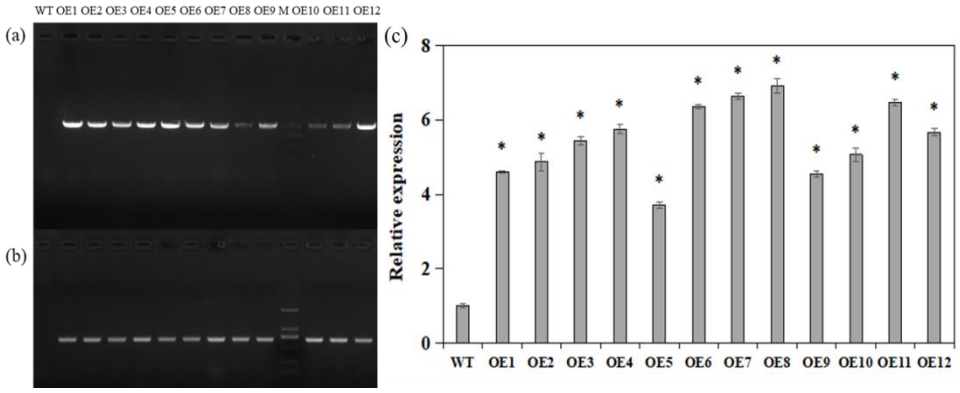

Figure S3 Identification of *pagHyPRP1* OE lines by PCR and reverse transcription quantitative PCR (RT-qPCR). PCR confirmation of 12 OE lines with pROKII-1 (a) and pROKII-2 (b). OE: overexpression, WT: wild type; M: 2000 bp DNA markers. (c) RT-qPCR analysis of *pagHyPRP1*expression level in OE lines. The bars represent the means ± the standard deviation (SD) (n = 3) * indicates significant differences between OE lines compared with the WT (*$P < 0.05$).

Table S1 Primer sequences used in this study.

Genes	Forward and reverse primers (5'–3')	
Primers used for RT-qPCR		
PagHyPRP1	CCTAAAGCTCCTATTACACTCCCTC	TAGCCCACCAAGAAGATCCAC
SOS1	ACAAACCAAGGGAACGTGAG	GATCGCTTGACTTGGCTACC
NHX1	CACACACCAGAAAGCTGCAT	GGAGCACCTTCTCCAACTGA
HKT1	TATGCCAACAAAGCAACAGG	CCAGTTGAGAACCCGACATT
AKT1	TTGCCCAGAAAAGGAAGAAG	TCCATCAGTGGCAAATACGA
PMA	TGACATATGTGCCGCTTGAT	GTGGGAGGTCTCAGGAGGTT
CPK1	GATCTGATGGATGCTGCTGA	ATCAAGGTGGAGCTCGCTTA
RBOHF	AACAAGGGAGCAGGGTTCTT	ACCGTTTTTCGCATGGTTTA
Actin	CATCCAGGCTGTCCTTTCCC	AACGAAGGATGGCGTGTGG
Primers used for identify *paghyprp1* mutant lines		
U6	TGTCCCAGGATTAGAATGATTAGGC	CATCGGAACTGCAAAACTCA
Cas9	ATCGTGGACCTGCTGTTCAAGAC	TACAGGTACAGCTTCTCGTTCTGCAG
Kan	ATGGGGATTGAACAAGATGGATTGC	TCAGAAGAACTCGTCAAGAAGGCGA
Primers used for identify OE lines		
pROKII-1	AGACGTTCCAACCACGTCTT	CCAGTGAATTCCCGATCTAG
pROKII-2	TTTCATTTGGAGAGAACACG	TGCCAAATGTTTGAACGATC
Primers used for identify *PagHyPRP1A* and *PagHyPRP1B* targeted sites		
PagHyPRP1A	CTCCACAAACTATACCACTCTG	AAATCCTTGCGCATAGGCTC
PagHyPRP1B	CGGTATAGGTACCGAGAGTGAACGGTACC ATGGATTCTACCAAAATTTCAGC	GCCAGGTAAAGTGAAGAACGTG
Primers used for vector construction		
Constructs	**Forward and reverse primers (5'–3')**	
pHZM58-	ATATATGGTCTCGGCAGCCGCCCCAACTCT TGACTGGTTTTAGAGCTAGAAATAGC	ATTATTGGTCTCGAAACCAAGAACCACA GTCAAGAGTGCACCAGCCGGGAATC

PagHyPRP1		
pROKII-*PagHyPRP1*	CGGGGTACCATGGATTCTACCAAAATTTCA GC	CGAGCTCCTAGAGAGAGCAAGTGTAAC CAG

References

Alnayef, M., Solis, C., Shabala, L., Ogura, T., Chen, Z., Bose, J., Maathuis, F. *et al*. (2020). Changes in expression level of *OsHKT1; 5* alters activity of membrane transporters involved in K+ and Ca2+ acquisition and homeostasis in salinized rice roots. *Int. J. Mol. Sci.* **21**(14), 4882.

Ali, A., Maggio, A., Bressan, R.A. and Yun, D.J. Role and functional differences of *HKT1-Type* transporters in plants under salt stress. *Int. J. Mol. Sci.* **20**, 1059.

An, Y., Zhou, Y., Han, X., Shen, C., Wang, S., Liu, C., Yin, W. *et al*. (2020) The GATA transcription factor GNC plays an important role in photosynthesis and growth in poplar. *J Exp Bot.* **71**, 1969-1984.

Azeez, A. and Busov, V. (2021). CRISPR/Cas9□mediated single and biallelic knockout of poplar *STERILE APETALA* (*PopSAP*) leads to complete reproductive sterility. *Plant Biotechnol. J.* **19**, 23–25.

Bahrun, A., Jensen, C.R., Asch, F. and Mogensen, V.O. (2002). Drought-induced changes in xylem pH, ionic composition, and ABA concentration act as early signals in field-grown *maize* (Zea mays L.). *J. Exp. Bot.* **53**, 251-263.

Banday, Z., Cecchini, N., Speed, D., Scott, A., Parent, C., Hu, C. T., *.et al*. (2022). Friend or foe: Hybrid proline-rich proteins determine how plants respond to beneficial and pathogenic microbes. *Plant physiology*, **190**(1), 860-881.

Barragán, V., Leidi, E. O., Andrés, Z., Rubio, L., De Luca, A., Fernández, J. A., Cubero, B. *et al*. (2012) Ion exchangers *NHX1* and *NHX2* mediate active potassium uptake into vacuoles to regulate cell turgor and stomatal function in *Arabidopsis*. *Plant Cell.* **24**, 1127-1142.

Bassil, E. and Blumwald, E. (2014) The ins and outs of intracellular ion homeostasis: NHX-type cation/H^+ transporters. *Curr. Opin. Plant Biol*. **22**, 1–6.

Bassil, E., Zhang, S., Gong, H., Tajima, H. and Blumwald, E. (2019) Cation specificity of vacuolar NHX-type cation/H^+ antiporters. *Plant Physiol*. **179**, 616–629.

Beffagna, N., Buffoli, B. and Busi, C. (2005) Modulation of reactive oxygen species production during osmotic stress in Arabidopsis thaliana cultured cells: involvement of the plasma membrane Ca^{2+}-ATPase and H^+-ATPase. *Plant Cell Physiol*. **46**, 1326-1339.

Boscari, A., Clement, M., Volkov, V., Golldack, D., Hybiak, J., Miller, A.J., Amtmann, A. *et al*. (2009) Potassium channels in barley: cloning, functional characterization and expression analyses in relation to leaf growth and development. *Plant Cell Environ*. **32**, 1761–1777.

Bowler, C. and Fluhr, R. (2000) The role of calcium and activated oxygens as signals for controlling cross-tolerance. *Trends Plant Sci*. **5**, 241-246.

Cao, S., Wang, C., Ji, H., Guo, M., Yang, C., Cheng, Y. and Cheng, J. (2021) Functional characterisation of the poplar atypical aspartic protease gene *PtAP66* in wood secondary cell wall deposition. *Forests*. **12**, 1002.

Chen, K., Wang, Y., Zhang, R., Zhang, H. and Gao, C. (2019) CRISPR/Cas genome editing and precision plant breeding in agriculture. *Annu Rev Plant Biol.* **70**, 667-697.

Chen, X., Ding, Y., Yang, Y., Song, C., Wang, B., Yang, S., Guo, Y. *et al*. (2021) Protein kinases in plant responses to drought, salt, and cold stress. *J Integr Plant Biol.* **63**, 53-78.

Coelho, S.M., Taylor, A.R., Ryan, K.P., Sousa-Pinto, I., Brown, M.T. and Brownlee, C. (2002) Spatiotemporal patterning of reactive oxygen production and Ca^{2+} wave propagation in fucus rhizoid cells. *Plant Cell.* **14**, 2369-81.

Cong, L., Ran, F., Cox, D., Lin, S., Barretto, R., Habib, N., Hsu, P.D. *et al*. (2013). Multiplex genome engineering using CRISPR/Cas systems. *Science,* **339**, 819-823.

de Vries, L., Brouckaert, M., Chanoca, A., Kim, H., Regner, M.R., Timokhin, V.I., Sun, Y. *et al*. (2021) CRISPR-Cas9 editing of CAFFEOYL SHIKIMATE *ESTERASE* 1 and 2 shows their importance and partial redundancy in lignification in Populus tremula×P.alba. *Plant Biotechnol. J*. **19**, 2221-2234.

Debbarma, J., Sarki, Y.N., Saikia, B., Boruah, H.P.D., Singha, D.L. and Chikkaputtaiah, C. (2019) Ethylene Response Factor (ERF) family proteins in abiotic stresses and CRISPR-Cas9 genome editing of ERFs for multiple abiotic stress tolerance in crop plants: a review. *Mol Biotechnol*. **61**, 153-172.

Ding, C., Zhang, W., Li, D., Dong, Y., Liu, J., Huang, J., and Su, X. (2020) Effect of overexpression of jerfs on intracellular k^+/na^+ balance in transgenic poplar (populus alba ×p. berolinensis) under salt stress. *Front Plant Sci*. **11**, 1192.

Dodd, A.N., Kudla, J. and Sanders, D. (2010) The language of calcium signaling. *Annu Rev Plant Biol.* **61**, 593-620.

Dong, Q., Wallrad, L., Almutairi, B.O. and Kudla, J. (2022) Ca^{2+} signaling in plant responses to abiotic stresses. *J Integr Plant Biol.* **64**, 287-300.

Elorriaga, E., Klocko, A.L., Ma, C., Du Plessis, M., An, X., Myburg, A.A. and Strauss, S.H. (2021). Genetic containment in vegetatively propagated forest trees: CRISPR disruption of LEAFY function in Eucalyptus gives sterile indeterminate inflorescences and normal juvenile development. *Plant Biotechnol. J.* **19**, 1743-1755.

Fan, D., Wang, X., Tang, X., Ye, X., Ren, S., Wang, D. and Luo, K. (2018) Histone *H3K9* demethylase *JMJ25* epigenetically modulates anthocyanin biosynthesis in poplar. *Plant J*. **96**, 1121-1136.

Fellenberg, C., Corea, O., Yan, L.H., Archinuk, F., Piirtola, E.M., Gordon, H., Reichelt, M. *et al*. (2020) Discovery of salicyl benzoate UDP-glycosyltransferase, a central enzyme in poplar salicinoid phenolic glycoside biosynthesis. *Plant J*. **102**, 99-115.

Feng, X., Liu, W., Qiu, C., Zeng, F., Wang, Y., Zhang, G., Chen, Z. *et al*. (2020) *HvAKT2* and *HvHAK1* confer drought tolerance in barley through enhanced leaf mesophyll H^+ homoeostasis. *Plant Biotechnol. J*. **18**, 1683-1696.

Feng, X., Liu, W., Zeng, F., Chen, Z., Zhang, G. and Wu, F. (2016) K^+ Uptake, H^+-ATPase pumping activity and Ca^{2+} efflux mechanism are involved in drought tolerance of barley. *Environ. Exp. Bot*. **129**, 57-66.

Gill, S.S. and Tuteja, N. (2010) Reactive oxygen species and antioxidant machinery in abiotic stress tolerance in crop plants. *Plant Physiol Biochem*. **48**, 909-930.

Gilroy, S., Białasek, M., Suzuki, N., Górecka, M., Devireddy, AR., Karpiński, S. and Mittler, R. (2016) ROS, calcium, and electric signals: key mediators of rapid systemic signaling in plants. *Plant Physiol.* **171**, 1606-15.

Gong, Z., Xiong, L., Shi, H., Yang, S., Herrera-Estrella, L., Xu, G., Chao, Y. *et al.* (2020) Plant abiotic stress response and nutrient use efficiency. *Sci. China Life Sci*. **63**, 635-674.

He, F., Wang, H.L., Li, H.G., Su, Y., Li, S., Yang, Y., Feng, C.H. et al. (2018) *PeCHYR1*, a ubiquitin E3 ligase from *Populus* euphratica, enhances drought tolerance via ABA-induced stomatal closure by ROS production in Populus. *Plant Biotechnol. J.* **16**, 1514–1528.

Hua, K., Zhang, J., Botella, J., Ma, C., Kong, F., Liu, B. and Zhu, J. (2019) Perspectives on the application of genome-editing technologies in crop breeding. *Mol Plant,* **12**, 1047-1059.

Jia, H. and Wang, N. (2020). Generation of homozygous canker-resistant citrus in the T0 generation using CRISPR-SpCas9p. *Plant Biotechnol. J*. **18**, 1990.

Jia, H., Zhang, Y., Orbović, V., Xu, J., White, F.F., Jones, J.B. and Wang, N. (2017) Genome editing of the disease susceptibility gene *CsLOB1* in citrus confers resistance to citrus canker. *Plant Biotechnol. J.* **15**, 817-823.

Jia, W. and Davies, W.J., (2007) Modification of leaf apoplastic pH in relation to stomatal sensitivity to root-sourced abscisic acid signals. *Plant Physiol.* **143**, 68–77.

Jiang, Y., Guo, L., Ma, X., Zhao, X., Jiao, B., Li, C. and Luo, K. (2017) The *WRKY* transcription factors *PtrWRKY18* and *PtrWRKY35* promote Melampsora resistance in Populus. *Tree Physiol.* **37**, 665-675.

Kadota, Y., Shirasu, K. and Zipfel, C. (2015) Regulation of the NADPH oxidase RBOHD during plant immunity. *Plant Cell Physiol.* **56**, 1472-1480.

Kapoor, R., Kumar, G., Arya, P., Jaswal, R., Jain, P., Singh, K. and Sharma, T.R. (2019) Genome-wide analysis and expression profiling of rice Hybrid Proline-Rich proteins in response to biotic and abiotic stresses, and hormone treatment. *Plants (Basel)*. **8**, 43.

Li, D., Yang, J., Pak, S., Zeng, M., Sun, J., Yu, S., He, Y. et al. (2022) *PuC3H35* confers drought tolerance by enhancing lignin and proanthocyanidin biosynthesis in the roots of Populus ussuriensis. *New Phytol.* **233**, 390-408.

Li, J., Guo, Y. and Yang, Y. (2022) The molecular mechanism of plasma membrane H^+-ATPases in plant responses to abiotic stress. *J Genet Genomics.* **49**, 715-725.

Li, J., Ouyang, B., Wang, T., Luo, Z., Yang, C., Li, H., Sima, W. et al. (2016) *HyPRP1* gene suppressed by multiple stresses plays a negative role in abiotic stress tolerance in tomato. *Front Plant Sci.* **7**, 967.

Li, L., Xing, J., Ma, H., Liu, F. and Wang, Y. (2021b) In situ determination of guard cell ion flux underpins the mechanism of ABA-mediated stomatal closure in *barley* plants exposed to PEG-induced drought stress. *Environmental and Experimental Botany*, **187**, 104468.

Li, R., Zhang, J., Wu, G., Wang, H., Chen, Y. and Wei, J. (2012). *HbCIPK2*, a novel CBL-interacting protein kinase from halophyte *Hordeum brevisubulatum*, confers salt and osmotic stress tolerance: *HbCIPK2* plays a role in salt and drought tolerance. *Plant, Cell Environ.* **35**, 1582–1600.

Li, S., Lin, Y.J., Wang, P., Zhang, B., Li, M., Chen, S., Shi, R. *et al.* (2019) The *AREB1* transcription factor influences histone acetylation to regulate drought responses and tolerance in *Populus trichocarpa*. *Plant Cell.* **31**, 663-686.

Liu, B., Wang, L., Zhang, J., Li, J., Zheng, H., Chen, J. and Lu, M. (2014) WUSCHEL-related Homeobox genes in *Populus tomentosa*: diversified expression patterns and a functional similarity in adventitious root formation. *BMC Genom.* **15**, 296.Liu, L., Song, W., Huang, S., Jiang, K., Moriwaki, Y., Wang, Y., Men, Y. *et al.* (2022) Extracellular pH sensing by plant cell-surface peptide-receptor complexes. *Cell*, **185**, 3341-3355.

Liu, S., Li, C., Wang, H., Wang, S., Yang, S., Liu, X., Yan, J. *et al.* (2020). Mapping regulatory variants controlling gene expression in drought response and tolerance in maize. *Genome Biol.* **21**, 163.

Liu, Z., Wang, P., Zhang, T., Li, Y., Wang, Y. and Gao, C. (2018) Comprehensive analysis of *BpHSP* genes and their expression under heat stresses in *Betula platyphylla*. *Environ Exp Bot.* **152**, 167-176.

Liu, Z., Xie, Q., Tang, F., Wu, J., Dong, W., Wang, C. and Gao, C. (2021a). The ThSOS3 gene improves the salt tolerance of transgenic *Tamarix hispida* and *Arabidopsis thaliana*. *Front Plant Sci. 11*, 597480.

Liu, Z., Li, X., Zhang, T., Wang, Y., Wang, C. and Gao, C.Q. (2021b) Overexpression of *ThMYB8* mediates salt stress tolerance by directly activating stress-responsive gene expression. *Plant Science*, **302**, 110668.

Livak, K. J. and Schmittgen, T. D. (2001) Analysis of relative gene expression data using real-time quantitative PCR and the 2-11CT Method. *Methods,* **25**, 402–408.

Ma, X., Li, J., Deng, C., Sun, J., Liu, J., Li, N., Chen, S. *et al.* (2020a) Nacl-altered oxygen flux profiles and h^+-atpase activity in roots of two contrasting poplar species. *Tree Physiology.* **41**(5).

Ma, Y., Wu, T., Zhong, G. and Zheng, Y. (2020b) Overexpression of a new proline-rich protein encoding Gene *CsPRP4* increases starch accumulation in Citrus. *Sci Hortic.* **260**, 108744.

Mahi, H.E., Pérez-Hormaeche, J., Luca, A.D., Villalta, I., Espartero, J., Gámez-Arjona, F., Bundó, M. *et al.* (2019). A critical role of sodium flux via the plasma membrane Na^+/H^+ exchanger *SOS1* in the salt tolerance of *rice*. *Plant Physiol.* **180**, 1046-1065.

Mak, M., Babla, M., Xu, S., O'Carrigan, A., Liu, X., Gong, Y., Holford, P. *et al.* (2014) Leaf mesophyll K^+, H^+ and Ca^{2+} fluxes are involved in drought-induced decrease in photosynthesis and stomatal closure in *soybean*. *Environ. Exp. Bot.* **98**, 1-12.

Marino, D., Dunand, C., Puppo, A. and Pauly, N. (2012) A burst of plant *NADPH* oxidases. *Trends Plant Sci.* **17**, 9-15.

Mellacheruvu, S., Tamirisa, S., Vudem, D.R. and Khareedu, V.R. (2016) Pigeonpea Hybrid-Proline-Rich Protein (CcHyPRP) confers biotic and abiotic stress tolerance in transgenic rice. *Front Plant Sci.* **6**, 1167.

Ming, M., Long, H., Ye, Z., Pan, C., Chen, J., Tian, R., Sun, C. *et al.* (2022) Highly efficient CRISPR systems for loss-of-function and gain-of-function research in pear calli. *Hortic Res.* **30**, 9.

Nawaz, G., Han, Y., Usman, B., Liu, F., Qin, B. and Li, R. (2019) Knockout of *OsPRP1*, a gene encoding proline-rich protein, confers enhanced cold sensitivity in rice (*Oryza sativa* L.) at the seedling stage. *3 Biotech.* **7**, 254.

Nayeri, S., Baghban, K.B., Ahmadikhah, A. and Mahna, N. (2022) CRISPR/Cas9-mediated P-CR domain-specific engineering of CESA4 heterodimerization capacity alters cell wall architecture and improves saccharification efficiency in poplar. *Plant Biotechnol. J.* **20**, 1197-1212.

Pak, S. and Li, C. (2022). Progress and challenges in applying CRISPR/Cas techniques to the genome editing of trees. *Forestry Research,* **2**, 0–0.

Peng, A., Chen, S., Lei, T., Xu, L.,He, Y., Wu, L., Yao, Y. *et al.* (2017) Engineering canker-resistant plants through crispr/cas9□targeted editing of the susceptibility gene cslob1 promoter in citrus. *Plant Biotechnol. J.* **15**, 1509-1519.

Peng, T., Jia, M.M. and Liu, J.H. (2015) RNAi-based functional elucidation of *PtrPRP*, a gene encoding a hybrid proline rich protein, in cold tolerance of *Poncirus trifoliata*. *Front Plant Sci.* **6**, 808.

Pompili, V., Dalla, C.L., Piazza, S., Pindo, M. and Malnoy, M. (2020) Reduced fire blight susceptibility in apple cultivars using a high-efficiency CRISPR/Cas9-FLP/FRT-based gene editing system. *Plant Biotechnol. J.* **18**, 845-858.

Priyanka, B., Sekhar, K., Reddy, V.D. and Rao, K.V. (2010) Expression of pigeonpea hybrid-proline-rich protein encoding gene (CcHyPRP) in yeast and Arabidopsis affords multiple abiotic stress tolerance. *Plant Biotechnol. J.* **8**, 76-87.

Ren, C., Guo, Y., Kong, J., Lecourieux, F., Dai, Z., Li, S. and Liang, Z. (2020) Knockout of *VvCCD8* gene in grapevine affects shoot branching. *BMC Plant Biol.* **20**, 47

Saikia, B., Debbarma, J., Maharana, J., Singha, D.L., Velmuruagan, N., Dekaboruah, H., Arunkumar, K.P. *et al.* (2020a) *SlHyPRP1* and *DEA1*, the multiple stress responsive eight-cysteine motif family genes of tomato (*Solanum lycopersicum* L.) are expressed tissue specifically, localize and interact at cytoplasm and plasma membrane in vivo. *Physiol Mol Biol Plants*. **26**, 2553-2568.

Saikia, B., Singh, S., Debbarma, J., Velmurugan, N., Dekaboruah, H., Arunkumar, K.P. and Chikkaputtaiah, C. (2020b) Multigene CRISPR/Cas9 genome editing of hybrid proline rich proteins (HyPRPs) for sustainable multi-stress tolerance in crops: the review of a promising approach. *Physiol Mol Biol Plants*. **5**,

857-869.

Sewelam, N., Kazan, K and Schenk, P.M. (2016) Global plant stress signaling: reactive oxygen species at the cross-road. *Front Plant Sci.* **7**, 187.

Shabala, L., Zhang, J., Pottosin, I., Bose, J., Zhu, M., Fuglsang, A.T., Velarde- Buendia, A. *et al.* (2016) Cell-type-specific H^+-ATPase activity in root tissues enables K^+ retention and mediates acclimation of barley (*Hordeum vulgare*) to salinity stress. *Plant Physiol.* **172**, 2445-2458

Shelake, R., Kadam, U.S., Kumar, R., Pramanik, D., Singh, A.K. and Kim, J.Y. (2022). Engineering drought and salinity tolerance traits in crops through CRISPR-mediated genome editing: Targets, tools, challenges, and perspectives. *Plant Commun.* 100417.

Shi, H., Ishitani, M., Kim, C. and Zhu, J. (2000) The *Arabidopsis thaliana* salt tolerance gene *SOS1* encodes a putative Na^+/H^+ antiporter. *Proc Natl Acad Sci USA*. **97**, 6896-901.

Shi, J., Gao, H., Wang, H., Lafitte, H.R., Archibald, R.L., Yang, M., Hakimi, S. M. *et al.* (2017). *ARGOS8* variants generated by CRISPR-Cas9 improve maize grain yield under field drought stress conditions. *Plant Biotechnol. J.* **15**, 207–216.

Sklodowski, K., Riedelsberger, J., Raddatz, N., Riadi, G., Caballero, J., Chérel, I., Schulze, W. *et al.* (2017) The receptor-like pseudokinase *MRH1* interacts with the voltage-gated potassium channel *AKT2*. *Sci Rep*. **7**, 44611.

Su, N., Wu, Q., Chen, J., Shabala, L., Mithöfer, A., Wang, H. and Qu, M. *et al*. (2019) GABA operates upstream of H^+-ATPase and improves salinity tolerance in *Arabidopsis* by enabling cytosolic K^+ retention and Na^+ exclusion. *J Exp Bot*. **70**, 6349-6361.

Sun, J., Chen, S., Dai, S., Wang, R., Li, N., Shen, X., Zhou, X. *et al*. (2009a) NaCl-induced alternations of cellular and tissue ion fluxes in roots of salt-resistant and salt-sensitive poplar species. *Plant Physiol*. **149**, 1141–1153

Sun, J., Dai, S., Wang, R., Chen, S., Li, N., Zhou, X., Lu, C. *et al*. (2009b) Calcium mediates root K^+/Na^+ homeostasis in poplar species differing in salt tolerance. *Tree Physiol.* **29**, 1175–1186

Sun, J., Li, L., Liu, M., Wang, M., Ding, M., Deng, S., Lu, C. *et al.* (2010a) Hydrogen peroxide and nitric oxide mediate K^+/Na^+ homeostasis and antioxidant defense in NaCl-stressed callus cells of two contrasting poplars. *Plant Cell Tiss Organ Cult.* **103**, 205-215.

Sun, J., Wang, M., Ding, M., Deng, S., Liu, M., Lu, C., Zhou, X. *et al*. (2010b) H_2O_2 and cytosolic Ca^{2+} signals triggered by the PM H-coupled transport system mediate K^+/Na^+ homeostasis in NaCl-stressed *Populus euphratica* cells. *Plant Cell Environ*. **33**, 943-958.

Tamura, K., Peterson, D., Peterson, N., Stecher, G., Nei, M. and Kumar, S. (2011) MEGA5: molecular evolutionary genetics analysis using maximum likelihood, evolutionary distance, and maximum parsimony methods. *Mol Biol Evol.* **28**, 2731–2739.

Tan, J., Zhuo, C. and Guo, Z. (2013) Nitric oxide mediates cold- and dehydration-induced expression of a novel *MfHyPRP* that confers tolerance to abiotic stress. *Physiol Plant*. **149**, 310-320.

Thompson, J.D., Gibson, T.J., Plewniak, F., Jeanmougin, F. and Higgins, D.G. (1997) The CLUSTAL_X windows interface: flexible strategies for multiple sequence alignment aided by quality analysis tools. *Nucleic Acids Res.* **25**, 4876-4882.

Tran, M.T., Doan, D.T.H., Kim, J., Song, Y.J., Sung, Y.W., Das, S., Kim, E.J. *et al*. (2021) CRISPR/Cas9-based precise excision of *SlHyPRP1* domain(s) to obtain salt stress-tolerant tomato. *Plant Cell Rep*. **40**, 999-1011.

Van Zelm, E., Zhang, Y. and Testerink, C. (2020). Salt tolerance mechanisms of plants. *Annu. Rev. Plant Biol.* **71**, 403-433.

Véry, A.A. and Sentenac, H. (2003) Molecular mechanisms and regulation of K^+ transport in higher plants. *Annual review of plant biology*, **54**, 575-603.

Wang, H., Yang, Q., Tan, S., Wang, T., Zhang, Y., Yang, Y., Yin, W. *et al*. (2022). Regulation of cytokinin biosynthesis using PtRD26pro□IPT module improves drought tolerance through PtARR10□PtYUC4/5□mediated reactive oxygen species removal in Populus. *J. Integr. Plant Biol*. **64**, 771–786.

Wang, L., Li, Z., Lu, M. and Wang, Y. (2017a) *ThNAC13*, a NAC transcription factor from *Tamarix hispida*, confers salt and osmotic stress tolerance to transgenic *Tamarix* and *Arabidopsis*. *Front. Plant Sci.* **8**, 635.

Wang, L., Ran, L., Hou, Y,, Tian, Q., Li, C., Liu, R. and Fan, D, Luo K. (2017b) The transcription factor *MYB115* contributes to the regulation of proanthocyanidin biosynthesis and enhances fungal resistance in *poplar*. *New Phytol.* **215**, 351-367.

Wang, L.Q., Wen, S.S., Wang, R., Wang, C., Gao, B. and Lu, M.Z. (2021) *PagWOX11*/12a activates *PagCYP736A12* gene that facilitates salt tolerance in poplar. *Plant Biotechnol. J*. **19**, 2249-2260.

Wang, W., Lin, T., Kieber, J. and Tsai, Y.C. (2019) Response Regulators 9 and 10 Negatively Regulate Salinity Tolerance in Rice. *Plant Cell Physiol.* **60**, 2549-2563.

Wang, X., Tu, M., Wang, D., Liu, J., Li, Y., Li, Z., Wang, Y. *et al*. (2018) CRISPR/Cas9-mediated efficient targeted mutagenesis in grape in the first generation. *Plant Biotechnol. J*. **16**, 844-855.

Wang, Y., Cao, Y., Liang, X., Zhuang, J., Wang, X., Qin, F. and Jiang, C. (2022) A dirigent family protein confers variation of Casparian strip thickness and salt tolerance in maize. *Nat Commun*. **13**, 2222.

Wu, H. (2018) Plant salt tolerance and Na^+ sensing and transport. *Crop J*. **6**, 215–225.

Xing, H.L., Dong, L., Wang, Z.P., Zhang, H.Y., Han, C.Y., Liu, B., Wang, X.C. *et al*. Chen QJ. (2014) A CRISPR/Cas9 toolkit for multiplex genome editing in plants. *BMC Plant Biology,***14**, 327.

Xu, C., Fu, X., Liu, R., Guo, L., Ran, L., Li, C., Tian, Q. *et al* . (2017) *PtoMYB170* positively regulates lignin deposition during wood formation in poplar and confers drought tolerance in transgenic Arabidopsis. *Tree Physiol*. **37**,1713-1726.

Xu, W., Cheng, H., Zhu, S., Cheng, J., Ji, H., Zhang, B., Cao, S. *et al*. (2021) Functional understanding of secondary cell wall cellulose synthases in populus trichocarpa via the cas9/grna-induced gene knockouts. *New Phytologist*. **231**, 1478-1495.

Xu, W.L., Zhang, D.J., Wu, Y.F., Qin, L.X., Huang, G.Q., Li, J., Li, L. *et al*.(2013) Cotton *PRP5* gene encoding a proline-rich protein is involved in fiber development. *Plant Mol Biol*. **82**, 353-365.

Xu, X., Xu, Z., Li, Z., Zakria, M., Zou, L. and Chen, G. (2021). Increasing resistance to bacterial leaf streak in rice by editing the promoter of susceptibility gene *OsSULRT3*; *6. Plant Biotechnol. J.*, **19**, 1101.

Xue, F., Liu, W., Qiu, C.W., Zeng, F., Wang, Y., Zhang, G., Wu, F. *et al*. (2020) HvAKT2 and HvHAK1hvhak1 confer drought tolerance in barley through enhanced leaf mesophyll H^+ homoeostasis. *Plant Biotechnol. J.*

Yang, G., Wang, Y., Xia, D., Gao, C., Wang, C. and Yang, C. (2014) Overexpression of a GST gene (*ThGSTZ1*) from *Tamarix hispida* improves drought and salinity tolerance by enhancing the ability to scavenge reactive oxygen species. *Plant Cell Tissue Organ Cult*. **117**, 99–112.

Yang, J., Zhang, Y., Wang, X., Wang, W., Li, Z., Wu, J., Wang, G. *et al*. (2018a) *HyPRP1* performs a role in negatively regulating cotton resistance to V. dahliae via the thickening of cell walls and ROS accumulation. *BMC Plant Biol*. **18**, 339.

Yang, L., Zhao, X., Ran, L., Li, C., Fan, D. and Luo, K. (2017) PtoMYB156 is involved in negative regulation of phenylpropanoid metabolism and secondary cell wall biosynthesis during wood formation in poplar. *Sci Rep*. **7**, 41209.

Yang, Y. and Guo, Y. (2018b). Elucidating the molecular mechanisms mediating plant salt-stress responses. *New Phytol.* **217**, 523.

Yeom, S., Seo, E., Oh, S., Kim, K.W. and Choi, D. (2012) A common plant cell-wall protein HyPRP1 has dual roles as a positive regulator of cell death and

a negative regulator of basal defense against pathogens. *Plant J*. **69**, 755–768.

Yin, X., Xia, Y., Xie, Q., Cao, Y., Wang, Z., Hao, G. Song, J. *et al.* (2020b). The protein kinase complex *CBL10-CIPK8-SOS1* functions in *Arabidopsis* to regulate salt tolerance. *J. Exp. Bot.* **71**, 1801–1814.

Zhang, H., Deng, C., Yao, J., Zhang, Y.L., Zhang, Y.N., Deng, S., Zhao, N. *et al*. (2019a) Molecular sciences *populus euphratica* jrl mediates aba response, ionic and ros homeostasis in arabidopsis under salt stress. *Int J Mol Sci*. **20**, 815.

Zhang, H., Zhu, J., Gong, Z.and Zhu, J. K. (2022). Abiotic stress responses in plants. *Nature Reviews Genetics,* 23(2), 104-119.

Zhang, T., Li, Y., Kang, Y., Wang, P., Li, W., Yu, W., Zhou, Y. *et al*. (2022) The *Dendrobium catenatum DcCIPK24* increases drought and salt tolerance of transgenic *Arabidopsis*. *Industrial Crops and Products*, **187**, 115375.

Zhang, X., Liu, L., Chen, B., Qin, Z., Xiao, Y., Zhang, Y., Yao, R. et al. (2019b) Progress in Understanding the Physiological and Molecular Responses of Populus to Salt Stress. *Int J Mol Sci*. **20**, 1312.

Zhang, X., Shen, Z., Sun, J., Yu, Y., Deng, S., Li, Z., Sun, C. *et al*. (2015) NaCl-elicited, vacuolar Ca^{2+} release facilitates prolonged cytosolic Ca^{2+} signaling in the salt response of *Populus euphratica* cells. *Cell Calcium*. **57**, 348-365.

Zhang, Y., Wang, Y., Sa, G., Zhang, Y., Deng, J., Wang, M., Zhang, H. *et al*. (2017) Populus euphratica J3 mediates root K^+/Na^+ homeostasis by activating plasma membrane H+-ATPase in transgenic Arabidopsis under NaCl salinity. *Plant Cell Tiss Organ Cult.* **131**, 75-88.

Zhao, N., Zhu, H.P., Zhang, H.L., Sun, J., Zhou, J.C., Deng, C., Zhang, Y. et al. (2018). Hydrogen sulfide mediates K+ and Na+ homeostasis in the roots of saltresistant and salt-sensitive poplar species subjected to NaCl stress. *Front. Plant Sci*. **9**, 1366.

Zhao, S., Zhang, Q., Liu, M., Zhou, H., Ma, C. and W, P. (2021) Regulation of plant responses to salt stress. *Int. J. Mol. Sci.* **22**, 9.

Zhou, Y., Xu, S., Jiang, N., Zhao, X., Bai, Z., Liu, J., Yao, W. *et al*. (2022). Engineering of rice varieties with enhanced resistances to both blast and bacterial blight diseases via CRISPR/Cas9. *Plant Biotechnol. J.* **20**, 876-885.

Zhou, Y., Zhang, Y., Wang, X., Han, X., An, Y., Lin, S., Shen, C. et al. (2020) Root-specific NF-Y family transcription factor, *PdNF-YB21*, positively regulates root growth and drought resistance by abscisic acid-mediated indoylacetic acid transport in Populus. *New Phytol*. **227**, 407-426.

Zhu, J.K. (2016). Abiotic stress signaling and responses in plants. *Cell.* **167**, 313-324.